J. Fluid Mech. (1993), *vol.* 251, *pp.* 239–271

Double reflection of capillary/gravity waves by a non-uniform current: a boundary-layer theory

By KARSTEN TRULSEN AND CHIANG C. MEI

Department of Civil and Environmental Engineering, Massachusetts Institute of Technology, Cambridge, MA 02139, USA

(Received 2 July 1992 and in revised form 21 December 1992)

When a train of gravity waves encounters an opposing current, the wavelength is shortened and the waves may be reflected. If capillarity is included, the shortened waves may be reflected for a second time and experience further shortening. By this process the initially long gravity waves can be damped by viscosity quickly without breaking. In this paper a boundary-layer approximation is obtained close to the reflection points, and is matched to the ray approximations outside. This is then applied to the propagation of a wavepacket. Damping is accounted for in the ray solution and the result is compared to the undamped solution. The case where the two reflection points coalesce is also considered. It is found that as the separation between the reflection points decreases, the wavepacket appears to remain longer in the region of reflections relative to the width of this region.

1. Introduction

The evolution of short surface waves on a variable current or a long wave is important to the understanding of sea wave spectra, and to the proper interpretation of remote sensing records obtained by satellite. Modern theories on the dynamics of infinitesimal short gravity waves on longer waves or slowly varying currents was begun by Longuet-Higgins & Stewart (1960, 1961) and Bretherton & Garrett (1968). For cases without reflection, the short-wave envelope is known to obey the law of wave-action conservation. A more recent account, using a Hamiltonian formulation, can be found in Henyey *et al.* (1988), for the evolution of short gravity/capillary waves on two-dimensional long waves. Partial reflection of gravity waves by an opposing current was studied by Stiassnie & Dagan (1979). An asymptotic theory uniformly valid near and away from the reflection point has been given by Smith (1975) for pure gravity waves. While blocking (or reflection) of capillary waves by currents or long waves of finite amplitude has been anticipated by Phillips (1981), Shyu & Phillips (1990) have recently reported a more detailed linear analysis of the phenomenon near and away from the point of reflection (the simple turning point), by extending the work of Smith (1975) to include capillary effects. They first reduced the free-surface boundary condition to a third-order ordinary differential equation, which was factored and reduced further to the second-order Airy equation near a reflection point. The effects of viscosity were discussed in general terms.

Wave reflection on non-uniform currents is of great physical interest since it is accompanied by drastic shortening of wavelength, as a result of the combined influence of capillarity, gravity and current. The role of viscous dissipation can hence be greatly amplified, such that short waves can be completely damped out without the help of breaking (Phillips 1981). This phenomenon of shortening has been observed in

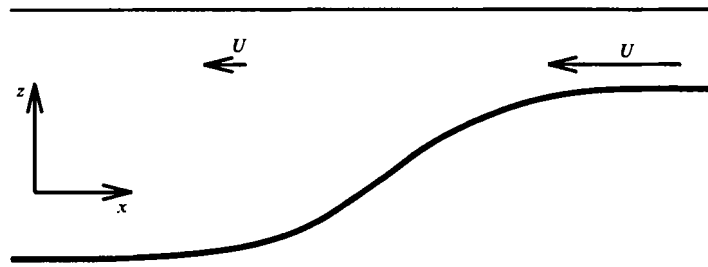

FIGURE 1. Geometry of the flow.

laboratory experiments. Specifically, Pokazeyev & Rozenberg (1983) conducted experiments for short waves on a weak current with speed between 4 and 21 cm/s over a sloping bottom. Packets of three to ten waves with central frequencies in the range of 2–11 Hz were sent towards an opposing current. Although they did not focus their attention on reflection, one of their experiments for waves of frequency 2 Hz showed double reflection and rapid spatial variation of wavelengths and amplitudes. The transmitted waves were found to be strongly attenuated. In a later experiment, Badulin, Pokazeyev & Rozenberg (1983) increased the opposing current speed to $U < 30$ cm/s and reduced the central frequency of the wavepackets to the range 1.5–3 Hz. Their attention was here on the propagation through the regions of reflection. They observed double reflection, accompanied by a drastic reduction of wavelength and amplitude attenuation. In these experiments, the separations between the two reflection points are typically not much greater than the local wavelengths.

The phenomenon of double reflection and drastic reduction of wavelength is best seen from the dispersion relation:

$$(\omega - \boldsymbol{k}\cdot\boldsymbol{U})^2 = gk + \frac{T}{\rho}k^3 \equiv \sigma^2. \tag{1.1}$$

Here σ is the intrinsic frequency, ω the absolute frequency, $\boldsymbol{k}$ the wavenumber vector, k its absolute magnitude $|\boldsymbol{k}|$, $\boldsymbol{U}$ the horizontal current velocity vector, g the gravitational acceleration, T the surface tension between water and air, and ρ the density of water. In the general case where the wave and the current are not in the same or opposite directions, the large variety of physical possibilities implied by (1.1) has been discussed by Basovich & Talanov (1977). Restricting our consideration to the collinear case for simplicity, we shall recapitulate some of the possible scenarios. Throughout the following we shall assume that the current flows from right to left towards increasing depth, see figure 1. The following cases can be distinguished.

Case 1. $\boldsymbol{k} = -k\hat{\boldsymbol{x}}$, i.e. $\boldsymbol{k}\cdot\boldsymbol{U} > 0$. Two branches exist for the square root in (1.1).

(*a*) Positive branch:

$$\sigma = \omega - |\boldsymbol{k}||\boldsymbol{U}| = \left(gk + \frac{T}{\rho}k^3\right)^{\frac{1}{2}}. \tag{1.2}$$

Since the intrinsic group velocity $c_g = \mathrm{d}\sigma/\mathrm{d}k > 0$, a long wave with crests propagating downstream will have its energy swept downstream. As the current gets weaker, the wavelength becomes shorter. There can be no reflection.

(*b*) Negative branch:

$$\sigma = \omega - |\boldsymbol{k}||\boldsymbol{U}| = -\left(gk + \frac{T}{\rho}k^3\right)^{\frac{1}{2}}. \tag{1.3}$$

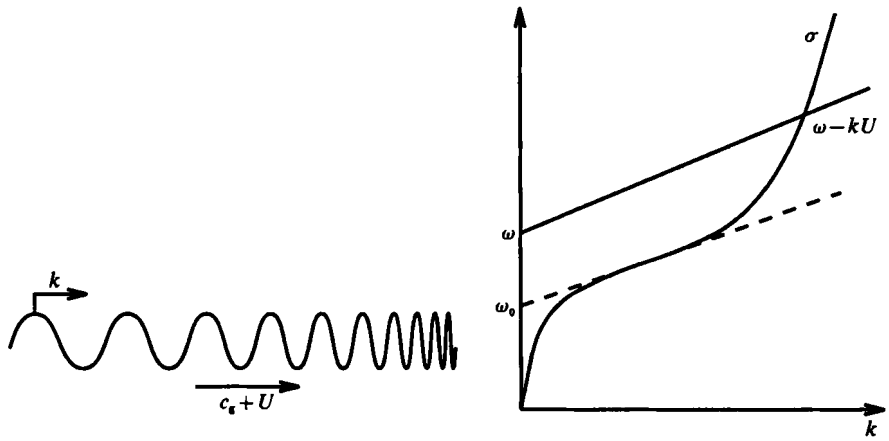

FIGURE 2. Case 2*a*. Graphic solution of dispersion relation and resulting wave, $\omega > \omega_0$.

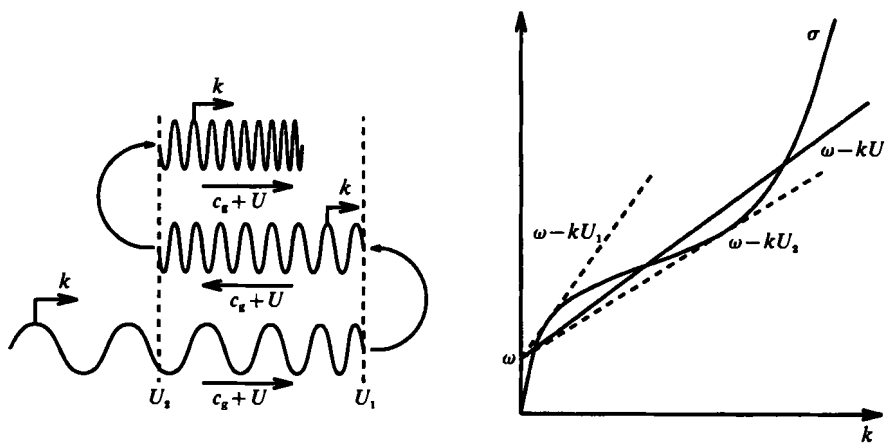

FIGURE 3. Case 2*b*. Graphic solution of dispersion relation and resulting wave, $\omega < \omega_0$.

In general there can be two wave trains, a longer wave propagating downstream and a shorter wave propagating upstream. As the current speed diminishes, the two waves coalesce to one; no downstream wave can exist for a weaker current. At the critical current intensity, energy is reflected upstream. This wave cannot exist on still water.

Case 2. $\boldsymbol{k} = k\hat{\boldsymbol{x}}$, i.e. $\boldsymbol{k}\cdot\boldsymbol{U} < 0$. Only the positive branch for the square root can be taken:

$$\omega + |\boldsymbol{k}||\boldsymbol{U}| = \left(gk + \frac{T}{\rho}k^3\right)^{\frac{1}{2}}. \tag{1.4}$$

Referring to figure 2 we define ω_0 to be the intersection of the frequency axis and the tangent to the intrinsic frequency curve at the inflexion point. There are two subcases.

(*a*) $\omega > \omega_0$. For any $|U|$ there is only one solution, as shown in figure 2. Because $\mathrm{d}\omega/\mathrm{d}k > 0$, a long wave propagating upstream will have its energy swept upstream. Since k increases with $|U|$ the wavelength is shortened as the crests advance into a stronger opposing current.

(*b*) $\omega < \omega_0$. For $U_2 < |U| < U_1$ three waves are possible for the same frequency, as shown in figure 3. A long wave originating downstream with wavenumber vector pointing upstream can be reflected twice at two different reflection points where

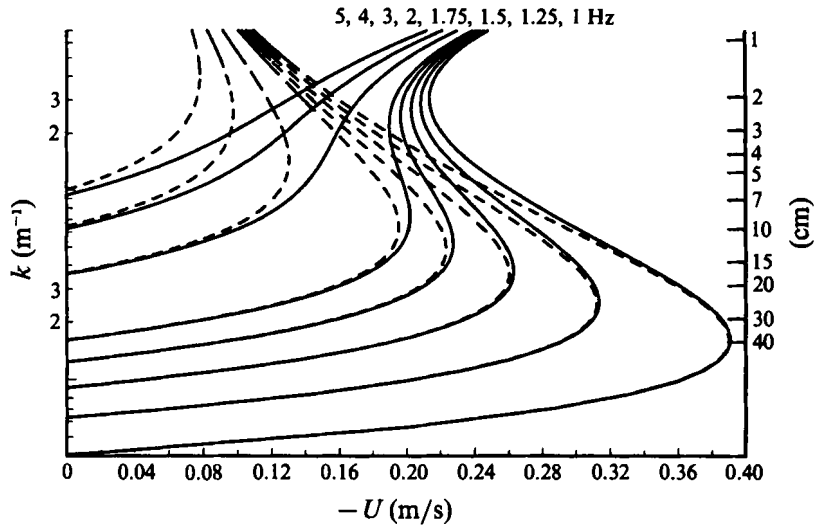

FIGURE 4. Wavenumber (m^{-1}) and wavelength (m) as a function of leftbound current velocity (m/s) for selected frequencies as shown. The solid lines show gravity/capillary theory, the broken lines show gravity theory without capillarity.

$|U| = U_1$ and $|U| = U_2$. The wavenumber vector always points upstream, while the wave energy is first swept upstream, then downstream, and finally upstream. Throughout this process the continuous shortening of the wavelength can be so drastic that fairly long gravity waves can be transformed into a train of capillary waves which are then damped without any breaking.

In the limiting case of $\omega \to \omega_0$, the two reflection points coalesce to one. We denote this as a triple turning point, to distinguish it from an ordinary turning point (or a reflection point). In physical dimensions achievable in the laboratory, solution curves of the dispersion relation for various frequencies and a given non-uniform current, are illustrated in figure 4.

In principle the theory of Shyu & Phillips (1990)† can be applied to the phenomenon of repeated reflections, if the reflection points are sufficiently far apart. In this paper, we wish to give an alternative theory, using a boundary-layer approach, for the repeated reflection of a packet of capillary–gravity waves on a non-uniform current by two well-separated reflection (blockage) points. Our main goal is however to extend the boundary-layer approach to the case where the two reflection points coalesce. Recent results by Paris (1991) on the Pearcey integral with complex parameters, will be used.

2. Scaling assumptions

Dividing (1.1) by ω, we get

$$1 = \left(\frac{gk}{\omega^2} + \frac{Tk^3}{\rho\omega^2}\right)^{\frac{1}{2}} + \frac{U}{c}, \tag{2.1}$$

where $c = \omega/k$ is the phase velocity of the wave. In order to deal with a wide range of wavelengths, we shall keep all three physical factors: gravity, capillarity and current.

† It is being applied by Yiqiang Zhang & O. M. Phillips (private communication) to related problems in gravity waves.

Mathematically this is done by formally allowing that gk/ω^2, $(T/\rho)k^3/\omega^2$ and U/c are all $O(1)$. Since $U/c \sim (g/A)^{\frac{1}{2}}/c \sim (kA)^{\frac{1}{2}}$, where A denotes the scale for the current set-down, it follows that $kA \sim O(1)$.

In many practical situations, current variations are accompanied by variations in depth. Let the depth and horizontal lengthscales be H and L, respectively, and assume

$$kH \sim O\left(\frac{1}{\epsilon}\right) \quad \text{and} \quad \frac{L}{A}, \quad kL \sim O\left(\frac{1}{\epsilon^2}\right) \tag{2.2}$$

where ϵ defined by

$$\epsilon = (\bar{k}L)^{-\frac{1}{2}} \tag{2.3}$$

is a small parameter. Hence the waves are on deep water, and variations in depth have a direct influence only on the current field.

Although the wavenumber varies widely, we shall choose that of the incident gravity wave as the characteristic wavenumber, i.e. $\bar{k} \equiv \bar{\omega}^2/g$. By this choice the actual ratio between the wave and current scales is never larger than $1/\bar{k}L = \epsilon^2$.

Let the short-wave amplitude be characterized-by a. The steepness ka is assumed to be so small that nonlinearity is unimportant over the propagation distance of $O(L)$. From existing theory of slowly varying waves, it is known that nonlinearity is not important over the distance $O(1/k(ka))$, but will be important over $O(1/k(ka)^2)$. Therefore we shall assume

$$ka \sim O(\epsilon^2). \tag{2.4}$$

Under these assumptions, it is convenient to employ multiple scale coordinates. For the waves the dimensional coordinates are (x, z, t), while for the current they are $(x_2 = \epsilon^2 x, z_1 = \epsilon z)$. Explicit expressions for an almost irrotational current over known bathymetry can easily be derived. However, the theory for the short waves is derived below by assuming that the current field is known *a priori*.

3. Approximate equations for the short wave

With an asterisk designating a physical variable, we let the velocity potential of the wave be ϕ^* and the wave-induced free-surface displacement be η^*. For the current the velocity components are denoted by (U^*, W^*) while the free-surface set-down is ζ^*. The total velocity field is then

$$\left(U^* + \frac{\partial \phi^*}{\partial x^*}\right)\hat{x} + \left(W^* + \frac{\partial \phi^*}{\partial z^*}\right)\hat{z},$$

while the total displacement of the free surface is $\zeta^* + \eta^*$.

Let $\bar{\omega}$ be the central frequency of the incident gravity wave from deep water, and $\bar{k} = \bar{\omega}^2/g$. We introduce the following normalizations for the current field:

$$x_2 = \epsilon^2 \bar{k} x^*, \quad z_1 = \epsilon \bar{k} z^*, \quad h = \epsilon \bar{k} h^*, \tag{3.1}$$

$$\zeta = \bar{k}\zeta^*, \quad U = (\bar{k}/g)^{\frac{1}{2}} U^*, \quad W = \frac{1}{\epsilon}(\bar{k}/g)^{\frac{1}{2}} W^*. \tag{3.2}$$

The following normalized variables are introduced for the short-wave field:

$$x = \bar{k}x^*, \quad z = \bar{k}z^*, \quad t = \bar{\omega}t^*, \quad K = k^*/\bar{k}, \tag{3.3}$$

$$\eta = (\bar{k}/\epsilon^2)\eta^*, \quad \phi = (\bar{k}/\epsilon^2)(k/g)^{\frac{1}{2}}\phi^*. \tag{3.4}$$

Assuming irrotationality, the dimensionless Laplace equation governing the wave field is

$$\frac{\partial^2\phi}{\partial x^2}+\frac{\partial^2\phi}{\partial z^2}=0 \quad \text{for} \quad -\frac{h}{\epsilon}<z<\zeta+\epsilon^2\eta. \tag{3.5}$$

The boundary condition on the bottom is

$$\frac{\partial\phi}{\partial z}=-\epsilon\frac{\partial\phi}{\partial x}\frac{\partial h}{\partial x_2} \quad \text{at} \quad z=-\frac{h}{\epsilon}. \tag{3.6}$$

On the free surface $z=\zeta+\epsilon^2\eta$, the kinematic condition for the total field reads

$$\epsilon\frac{\partial\eta}{\partial t}+\epsilon\left(U+\epsilon^2\frac{\partial\phi}{\partial x}\right)\left(\frac{\partial\zeta}{\partial x_2}+\frac{\partial\eta}{\partial x}\right)=W+\epsilon\frac{\partial\phi}{\partial z}, \tag{3.7}$$

while the dynamic condition reads

$$\epsilon^2\frac{\partial\phi}{\partial t}+\zeta+\epsilon^2\eta+\frac{1}{2}\left[\left(U+\epsilon^2\frac{\partial\phi}{\partial x}\right)^2+\left(\epsilon W+\epsilon^2\frac{\partial\phi}{\partial z}\right)^2\right]=\Gamma\frac{\epsilon^4\partial^2\zeta/\partial x_2^2+\epsilon^2\partial^2\eta/\partial x^2}{[1+\epsilon^4(\partial\zeta/\partial x_2+\partial\eta/\partial x)^2]^{\frac{3}{2}}}. \tag{3.8}$$

The following dimensionless quantity signifying surface tension has been introduced:

$$\Gamma=T\bar{k}^3/\rho\bar{\omega}^2. \tag{3.9}$$

We now Taylor-expand the free-surface conditions about the current set-down $z=\zeta$. Note that the current-related quantities are evaluated at $z_1=\epsilon\zeta+\epsilon^3\eta$, while wave-related quantities are evaluated at $z=\zeta+\epsilon^2\eta$. Let the current be weakly irrotational, such that

$$\frac{\partial U}{\partial z_1}-\epsilon^2\frac{\partial W}{\partial x_2}\leqslant O(\epsilon^2), \tag{3.10}$$

then

$$\begin{aligned} U|_{z_1=\epsilon\zeta+\epsilon^3\eta} &= U|_{z_1=\epsilon\zeta}+\epsilon^3\eta\left.\frac{\partial U}{\partial z_1}\right|_{z_1=\epsilon\zeta}+O(\epsilon^6) \\ &= U|_{z_1=\epsilon\zeta}+O(\epsilon^5). \end{aligned} \tag{3.11}$$

From the kinematic surface condition and the mass conservation equation for the current, we get

$$\begin{aligned} W|_{z_1=\epsilon\zeta+\epsilon^3\eta} &= \left[W+\epsilon^3\eta\frac{\partial W}{\partial z_1}+O(\epsilon^6)\right]_{z_1=\epsilon\zeta} \\ &= \left[\epsilon U\frac{\partial\zeta}{\partial x_2}-\epsilon^3\eta\frac{\partial U}{\partial x_2}+O(\epsilon^6)\right]_{z_1=\epsilon\zeta}. \end{aligned} \tag{3.12}$$

The wave velocity potential becomes

$$\phi|_{z=\zeta+\epsilon^2\eta}=\left[\phi+\epsilon^2\eta\frac{\partial\phi}{\partial z}+O(\epsilon^4)\right]_{z=\zeta}. \tag{3.13}$$

Note that in the surface conditions, differentiation must be performed first, before their values are evaluated on the surface. Thus, horizontal and time derivatives of ϕ must be taken before expansion about the current set-down.

After Taylor expansion, the kinematic free-surface condition becomes

$$\frac{\partial\eta}{\partial t}+U\frac{\partial\eta}{\partial x}-\frac{\partial\phi}{\partial z}+\epsilon^2\frac{\partial\zeta}{\partial x_2}\frac{\partial\phi}{\partial x}+\epsilon^2\frac{\partial U}{\partial x_2}\eta=-\epsilon^2\frac{\partial\phi}{\partial x}\frac{\partial\eta}{\partial x}+\epsilon^2\eta\frac{\partial^2\phi}{\partial z^2}+O(\epsilon^4)\quad\text{at}\quad z=\zeta. \tag{3.14}$$

Similarly, the dynamic free-surface condition is

$$\frac{\partial\phi}{\partial t}+\eta+U\frac{\partial\phi}{\partial x}-\Gamma\frac{\partial^2\eta}{\partial x^2}+\epsilon^2U\frac{\partial\zeta}{\partial x_2}\frac{\partial\phi}{\partial z}$$
$$=\epsilon^2\left[-\eta\frac{\partial^2\phi}{\partial t\,\partial z}-U\eta\frac{\partial^2\phi}{\partial x\,\partial z}-\frac{1}{2}\left(\frac{\partial\phi}{\partial x}\right)^2-\frac{1}{2}\left(\frac{\partial\phi}{\partial z}\right)^2\right]+O(\epsilon^3)\quad\text{at}\quad z=\zeta. \tag{3.15}$$

In summary, the short wave satisfies (3.5) in the fluid, (3.6) on the bottom and (3.14) and (3.15) on the curved surface $z=\zeta(x_2)$. Next, we shall seek information regarding the evolution of a slowly varying wavetrain which is proportional to $\exp\mathrm{i}(Kx-t)$. The terms linear in ϕ or η will contain this harmonic while the quadratic terms at $O(\epsilon^2)$ will give rise to zeroth and second harmonics. Hence the quadratic terms do not affect the first harmonic at order $O(\epsilon^2)$.

The linear wave solution is expected to attenuate exponentially in z, hence the fluid domain is well approximated by $-\infty<z<\zeta$ and the bottom condition may be replaced by

$$\partial\phi/\partial z\to 0\quad\text{as}\quad z\to-\infty. \tag{3.16}$$

4. Ray approximation for short waves away from points of reflection

In this section we present a ray approximation for waves far away from the reflection points. In principle, the results can be inferred from Shyu & Phillips (1990) and Henyey *et al.* (1988). Since the horizontal variation of the current has been assumed to have the characteristic scale $O(\epsilon^2x)$, it is natural to assume that the resulting modulation of the waves will be on the scales $x_2=\epsilon^2x$ and $t_2=\epsilon^2t$. First, we replace all x and t by x_2 and t_2 so that

$$\epsilon^4\frac{\partial^2\phi}{\partial x_2^2}+\frac{\partial^2\phi}{\partial z^2}=0\quad\text{for}\quad-\infty<z<\zeta, \tag{4.1}$$

$$\frac{\partial\phi}{\partial z}=0\quad\text{for}\quad z\to-\infty, \tag{4.2}$$

$$\epsilon^2\frac{\partial\eta}{\partial t_2}+\epsilon^2U\frac{\partial\eta}{\partial x_2}-\frac{\partial\phi}{\partial z}+\epsilon^4\frac{\partial\zeta}{\partial x_2}\frac{\partial\phi}{\partial x_2}+\epsilon^2\frac{\partial U}{\partial x_2}\eta=\text{h.o.t.}\quad\text{at}\quad z=\zeta, \tag{4.3}$$

$$\epsilon^2\frac{\partial\phi}{\partial t_2}+\epsilon^2U\frac{\partial\phi}{\partial x_2}+\eta-\epsilon^4\Gamma\frac{\partial^2\eta}{\partial x_2^2}+\epsilon^2U\frac{\partial\zeta}{\partial x_2}\frac{\partial\phi}{\partial z}=\text{h.o.t.}\quad\text{at}\quad z=\zeta, \tag{4.4}$$

where h.o.t. represents higher-order terms.

We now assume WKB-expansions of the form

$$\left.\begin{aligned}\phi&=(A+\epsilon^2A_2+\ldots)\exp(\mathrm{i}\epsilon^{-2}S)+\epsilon^2(\text{other harmonics})+\text{c.c.},\\ \eta&=(B+\epsilon^2B_2+\ldots)\exp(\mathrm{i}\epsilon^{-2}S)+\epsilon^2(\text{other harmonics})+\text{c.c.},\end{aligned}\right\} \tag{4.5}$$

where c.c. denotes complex conjugate and

$$\partial S/\partial x_2=K\quad\text{and}\quad\partial S/\partial t_2=-1. \tag{4.6}$$

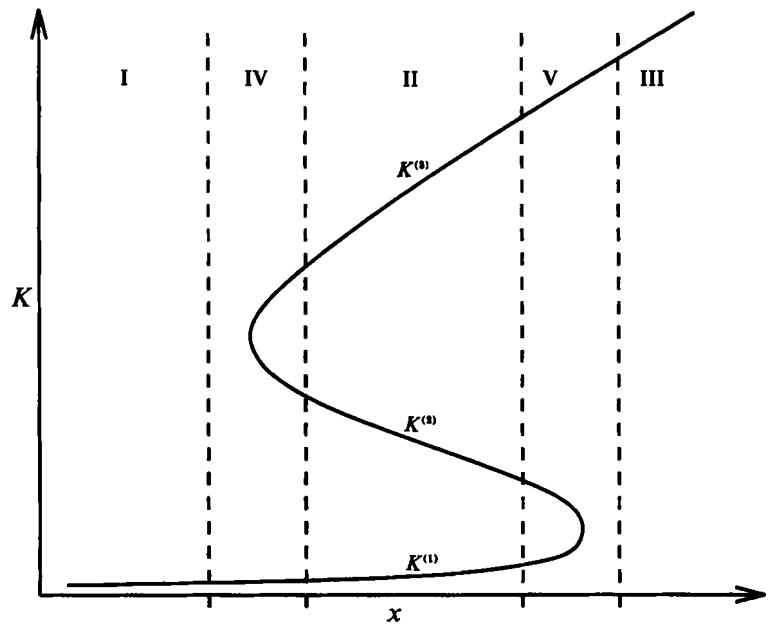

FIGURE 5. Sketch of the different regions of the wave development.

At the lowest order, $O(1)$, the problem is governed by

$$\partial^2 A/\partial z^2 - K^2 A = 0 \quad \text{for} \quad -\infty < z < \zeta, \tag{4.7}$$

$$\partial A/\partial z = 0 \quad \text{at} \quad z \to -\infty, \tag{4.8}$$

$$-\mathrm{i}B + \mathrm{i}KUB - \partial A/\partial z = 0 \quad \text{at} \quad z = \zeta, \tag{4.9}$$

$$-\mathrm{i}A + \mathrm{i}KUA + B + \Gamma K^2 B = 0 \quad \text{at} \quad z = \zeta. \tag{4.10}$$

The last two conditions can be combined to

$$\frac{\partial A}{\partial z} - \frac{K(1-KU)^2}{\sigma^2} A = 0, \tag{4.11}$$

where

$$\sigma \equiv (K + \Gamma K^3)^{\frac{1}{2}} \tag{4.12}$$

represents the intrinsic frequency of the wave.

We shall take the solution to be

$$A = -\frac{\mathrm{i}\sigma}{K} B \mathrm{e}^{K(z-\zeta)}, \quad \text{where} \quad B = B(x_2, t_2). \tag{4.13}$$

It readily follows that $K(x_2)$ is the solution of the dispersion relation

$$1 - KU = (K + \Gamma K^3)^{\frac{1}{2}} \quad \text{or} \quad \Gamma K^3 - U^2 K^2 + (2U+1)K - 1 = 0. \tag{4.14a, b}$$

Equation (4.14b) is a cubic equation for K with real coefficients. For a fixed Γ, K follows one of the curves in figure 4, which is plotted in physical variables and contrasted with a theory discounting surface tension. Assume that $U(x_2)$ varies monotonically in x_2. There are in general three real or one real and two complex-conjugate solutions, $K^{(1)}$, $K^{(2)}$ and $K^{(3)}$. With reference to figure 5, we divide the physical domain into five parts. In region I there is only one incident long wave $(K^{(1)}, B^{(1)})$, while in region III there is only one outgoing short wave $(K^{(3)}, B^{(3)})$. In

region II there can be three waves. The most general expression for the wave surface displacement is then

$$\eta(x_2, t_2) = \sum_{n=1}^{3} \left\{ B^{(n)}(x_2, t_2) \exp\left(\mathrm{i}\epsilon^{-2} \int^{x_2} K^{(n)} \, \mathrm{d}x_2 \right) + O(\epsilon^2) \right\} \exp(-\mathrm{i}\epsilon^{-2} t_2) + \text{c.c.} \quad (4.15)$$

Leaving the neighbourhoods of the isolated turning points IV and V to the next section, we first determine the amplitude B, the generic symbol for $B^{(1)}$, $B^{(2)}$ and $B^{(3)}$.

The second-order problem, $O(\epsilon^2)$, is

$$\frac{\partial^2 A_2}{\partial z^2} - K^2 A_2 = -\mathrm{i}\frac{\partial}{\partial x_2}(KA) - \mathrm{i}K\frac{\partial A}{\partial x_2} \quad \text{for} \quad -\infty < z < \zeta, \quad (4.16)$$

$$\partial A_2/\partial z = 0 \quad \text{at} \quad z \to -\infty, \quad (4.17)$$

$$\frac{\partial B}{\partial t_2} - \mathrm{i}B_2 + U\frac{\partial B}{\partial x_2} + \mathrm{i}KUB_2 - \frac{\partial A_2}{\partial z} + \mathrm{i}K\frac{\partial \zeta}{\partial x_2}A + \frac{\partial U}{\partial x_2}B = 0 \quad \text{at} \quad z = \zeta, \quad (4.18)$$

$$\frac{\partial A}{\partial t_2} - \mathrm{i}A_2 + U\frac{\partial A}{\partial x_2} + \mathrm{i}KUA_2 + B_2 - \mathrm{i}\Gamma\frac{\partial}{\partial x_2}(KB) - \mathrm{i}\Gamma K\frac{\partial B}{\partial x_2} + \Gamma K^2 B_2 + U\frac{\partial \zeta}{\partial x_2}\frac{\partial A}{\partial z} = 0$$

$$\text{at} \quad z = \zeta. \quad (4.19)$$

The last two equations can be combined by eliminating B_2, and the first-order result can further be used to substitute for A. The resulting surface condition is

$$\frac{\partial A_2}{\partial z} - KA_2 = 2\frac{\partial B}{\partial t_2} + U\frac{\partial B}{\partial x_2} + \sigma\frac{\partial \zeta}{\partial x_2}B + \frac{\partial U}{\partial x_2}B + \frac{KU}{\sigma}\frac{\partial}{\partial x_2}\left(\frac{\sigma}{K}B\right) + \frac{\Gamma K}{\sigma}\frac{\partial}{\partial x_2}(KB) + \frac{\Gamma K^2}{\sigma}\frac{\partial B}{\partial x_2}. \quad (4.20)$$

The problem for A_2 is seen to be an inhomogeneous version of the homogeneous problem for A. Therefore A_2 must satisfy a condition of solvability, which follows by Green's theorem,

$$\int_{-\infty}^{\zeta} \mathrm{d}z \left[A\left(\frac{\partial^2 A_2}{\partial z^2} - K^2 A_2\right) - A_2\left(\frac{\partial^2 A}{\partial z^2} - K^2 A\right) \right] = \left[A\frac{\partial A_2}{\partial z} - A_2\frac{\partial A}{\partial z} \right]_{-\infty}^{\zeta}. \quad (4.21)$$

After substituting (4.16)–(4.20) into this condition, we get the following condition for B:

$$\frac{\partial}{\partial x_2}\left\{\left(\frac{\sigma^2}{2K^2} + \frac{\sigma U}{K} + \Gamma K\right)B^2\right\} + \frac{\partial}{\partial t_2}\left\{\frac{\sigma}{K}B^2\right\} = 0. \quad (4.22)$$

Let us introduce the intrinsic group velocity

$$c_g \equiv \frac{\mathrm{d}\sigma}{\mathrm{d}K} = \frac{\sigma}{2K} + \frac{\Gamma K^2}{\sigma}, \quad (4.23)$$

so that we get

$$\frac{\partial}{\partial x_2}\left\{\frac{\sigma}{K}(c_g + U)B^2\right\} + \frac{\partial}{\partial t_2}\left\{\frac{\sigma}{K}B^2\right\} = 0. \quad (4.24)$$

This is the conservation law for wave action

$$\frac{\partial}{\partial x_2}\left\{\frac{E}{\sigma}(c_g + U)\right\} + \frac{\partial}{\partial t_2}\left\{\frac{E}{\sigma}\right\} = 0, \quad (4.25)$$

where $E = \rho\sigma^2 B^2/2K$ is the total energy. This equation has been deduced in similar contexts by Bretherton & Garrett (1968), Henyey *et al.* (1988) and Shyu & Phillips (1990).

As an application, we now seek a solution representing a wavepacket. Recall that c_g, U, K and σ are all independent of time. Upon multiplication of (4.24) by $c_g + U$, and introduction of $\psi = (c_g + U)\sigma B^2/K$, we write

$$\frac{\partial \psi}{\partial t_2} + (c_g + U)\frac{\partial \psi}{\partial x_2} = 0. \tag{4.26}$$

It follows that ψ is constant along the characteristic curve

$$t_2 - T = \int_X^{x_2} \frac{\mathrm{d}x_2}{c_g + U}, \tag{4.27}$$

where X and T are some reference values. Hence the solution for B becomes

$$B(x_2, t_2) = b\left(t_2 - \int_X^{x_2} \frac{\mathrm{d}x_2}{c_g + U}\right)\left(\frac{K}{\sigma(c_g + U)}\right)^{\frac{1}{2}}, \tag{4.28}$$

where b is the time-dependent boundary value of B at $x_2 = X$,

$$B(X, t_2) = b(t_2)\left(\frac{K}{\sigma(c_g + U)}\right)^{\frac{1}{2}}\Bigg|_{x_2 = X}. \tag{4.29}$$

Note that the solution breaks down at turning points where $c_g = -U$. To further examine its behaviour near the turning points, we rewrite the above square root as

$$\left|\frac{1}{\sigma^2/2K^2 + \sigma U/K + \Gamma K}\right|^{\frac{1}{2}} = \left|\frac{2K^2}{2\Gamma K^3 - U^2K^2 + 1}\right|^{\frac{1}{2}}. \tag{4.30}$$

Now the dispersion relation (4.14*b*) can be written in the form

$$\Gamma(K - K^{(1)})(K - K^{(2)})(K - K^{(3)}) = 0, \tag{4.31}$$

where $K^{(1)} < K^{(2)} < K^{(3)}$ denote the three (real) roots. It is clear that $1/\Gamma = K^{(1)}K^{(2)}K^{(3)}$ and $U^2/\Gamma = K^{(1)} + K^{(2)} + K^{(3)}$. Let us further assume, for illustration, that the wavenumber under consideration is $K = K^{(2)}$, corresponding to $B^{(2)}(x_2)$. We then get from (4.30)

$$B^{(2)}(x_2) = b\left(\frac{2K^{(2)}}{\Gamma(K^{(2)} - K^{(1)})(K^{(2)} - K^{(3)})}\right)^{\frac{1}{2}}. \tag{4.32}$$

It is clear that the ray theory solution is valid as long as $K^{(1)} \neq K^{(2)} \neq K^{(3)}$, and breaks down at the points where the dispersion has a double root, $K^{(1)} = K^{(2)}$ or $K^{(2)} = K^{(3)}$, or a triple root, $K^{(1)} = K^{(2)} = K^{(3)}$. The asymptotic behaviour of the amplitude near such points will depend on the multiplicity of the roots, as discussed separately in subsequent sections.

5. Inner solution near a simple turning point

In this section we shall rederive the theory of Shyu & Phillips by matched asymptotics for an isolated turning point and apply the results to the case with two well separated turning points.

Let us consider the neighbourhood of a simple turning point at $x_2 = x_0$ where there is a double root for the wavenumber, $K = K_0$. Thus two solution branches B^+ and B^-, with their respective wavenumbers K^+ and K^-, converge to K_0 at the turning point. In the following, we shall let indices $-$ and $+$ denote the longer and shorter waves, respectively, such that $K^- < K^+$. With this general convention, the theory is equally valid in both regions IV and V in figure 5.

Let us shift the origin by $\tilde{x} = x_2 - x_0$, and expand the current field in local expansions. We begin by noting that the current set-down can be expanded as

$$\zeta(x_2) = \zeta_0 + \tilde{x}\zeta_1 + O(\tilde{x}^2), \tag{5.1}$$

where $\zeta_0 \equiv \zeta$ and $\zeta_1 \equiv \partial\zeta/\partial x_2$, both evaluated at $x_2 = x_0$. The surface horizontal current can then be expanded as

$$U(x_2) = U_0 + \tilde{x}\frac{\partial U}{\partial x_2} + \epsilon\tilde{x}\zeta_1\frac{\partial U}{\partial z_1} + O(\tilde{x}^2), \tag{5.2}$$

where the terms on the right-hand side are evaluated at $z_1 = \epsilon\zeta_0$ and $x_2 = x_0$. Owing to the assumption that the current has weak vorticity,

$$\frac{\partial U}{\partial z_1} - \epsilon^2\frac{\partial W}{\partial x_2} \leqslant O(\epsilon^2), \tag{5.3}$$

we have $\partial U/\partial z_1 = O(\epsilon^2)$. If we define $U_1 \equiv \partial U/\partial x_2$ at $x_2 = x_0, z_1 = \epsilon\zeta_0$, the expansion for the surface horizontal current is

$$U(x_2) = U_0 + \tilde{x}U_1 + O(\tilde{x}^2, \epsilon^3\tilde{x}). \tag{5.4}$$

Suppose that the wavenumber behaves as $K = K_0 + R(\tilde{x})$ for small $\tilde{x}$, where $R(\tilde{x}) = o(1)$. Substituting these expansions into the dispersion relation (4.14*b*), and expanding for small $\tilde{x}$, we get

$$R^2(3\Gamma K_0 - U_0^2) + R^3\Gamma + 2U_1K_0\sigma_0\tilde{x} = O(\tilde{x}R), \tag{5.5}$$

where $\sigma_0 \equiv (K_0 + \Gamma K_0^3)^{\frac{1}{2}}$, and use has been made of the fact that $c_g \equiv \mathrm{d}\sigma/\mathrm{d}K = -U$ at $\tilde{x} = 0$. Clearly, the leading asymptotic behaviour for small $\tilde{x}$ is $R \sim \tilde{x}^{\frac{1}{2}}$. Consequently, the wavenumber can be expanded in half-powers of $\tilde{x}$,

$$K \sim K_0 + \alpha\tilde{x}^{\frac{1}{2}} + \beta\tilde{x}, \tag{5.6}$$

$$\text{where} \quad \alpha = \left(-\frac{2U_1K_0\sigma_0}{3\Gamma K_0 - U_0^2}\right)^{\frac{1}{2}} \quad \text{and} \quad \beta = \frac{U_1(5K_0^2U_0\Gamma - 2K_0\Gamma - 2K_0U_0^3 + U_0^2)}{(3K_0\Gamma - U_0^2)^2}. \tag{5.7}$$

Substitution of expansions (5.4) and (5.6) for U and K into (4.28) gives the inner approximation of the outer (ray) solution near the turning point,

$$\begin{aligned} B^{\pm}(\tilde{x}, t_2) &= b_{\pm}\left(t_2 - \int_{\tilde{x}_{\pm}}^{\tilde{x}} \frac{\mathrm{d}\tilde{x}}{c_g^{\pm} + U}\right)\left(\frac{K^{\pm}}{\sigma^{\pm}(c_g^{\pm} + U)}\right)^{\frac{1}{2}} \\ &\sim b_{\pm}\left(t_2 - \int_{\tilde{x}_{\pm}}^{\tilde{x}} \frac{\mathrm{d}\tilde{x}}{c_g^{\pm} + U}\right)\left(\left|-\frac{\alpha}{2\sigma_0U_1}\right|^{\frac{1}{2}}|\tilde{x}|^{-\frac{1}{4}} + O(\tilde{x}^{\frac{1}{4}})\right), \end{aligned} \tag{5.8}$$

where b_- and b_+ are the complex amplitudes of the incident and reflected waves, respectively, on the incidence side of the reflection point, and $\tilde{x}_{\pm}$ are the starting points for the time and phase integrals.

The evanescent modes on the opposite side of the reflection point are exponentially attenuated in $\tilde{x}$, and need not be taken into account for the present purposes.

From the inhomogeneous Laplace equation at $O(\epsilon^2)$, (4.16), the dominant behaviour at this order can be seen to be

$$A_2^{\pm} \sim B_2^{\pm} \sim O(\tilde{x}^{-\frac{3}{4}}). \tag{5.9}$$

Therefore the surface displacement on the incidence side of the singularity can be expanded as

$$\begin{aligned}\eta(\tilde{x}, t_2) &= B^- \exp\left(\mathrm{i}\epsilon^{-2}\left[\int_{\tilde{x}_-}^{\tilde{x}} K^- \,\mathrm{d}\tilde{x} - t_2\right]\right) + B^+ \exp\left(\mathrm{i}\epsilon^{-2}\left[\int_{\tilde{x}_+}^{\tilde{x}} K^+ \,\mathrm{d}\tilde{x} - t_2\right]\right) + O(\epsilon^2) \\ &\sim \left|-\frac{\alpha}{2\sigma_0 U_1}\right|^{\frac{1}{2}} |\tilde{x}|^{-\frac{1}{4}} \left\{ b_- \left[t_2 - \int_{\tilde{x}_-}^{\tilde{x}} \frac{\mathrm{d}\tilde{x}}{c_g^- + U}\right] \exp\left(\mathrm{i}\epsilon^{-2}\left[\int_{\tilde{x}_-}^{0} K^- \,\mathrm{d}\tilde{x} + K_0 \tilde{x} - \tfrac{2}{3}|\alpha \tilde{x}^3|^{\frac{1}{2}}\right]\right) \right. \\ &\quad \left. + b_+ \left(t_2 - \int_{\tilde{x}_+}^{\tilde{x}} \frac{\mathrm{d}\tilde{x}}{c_g^+ + U}\right) \exp\left(\mathrm{i}\epsilon^{-2}\left[\int_{\tilde{x}_+}^{0} K^+ \,\mathrm{d}\tilde{x} + K_0 \tilde{x} + \tfrac{2}{3}|\alpha \tilde{x}^3|^{\frac{1}{2}}\right]\right)\right\} \exp(-\mathrm{i}\epsilon^{-2} t_2).\end{aligned} \tag{5.10}$$

Higher powers of $\tilde{x}$ from $B^{\pm}$ will give contributions of $O(\tilde{x}^{\frac{1}{4}})$, while the $O(\epsilon^2)$ terms will give contributions of $O(\epsilon^2 \tilde{x}^{-\frac{5}{4}})$. Hence this one-term asymptotic expansion for the amplitude of the outer solution is valid for $\epsilon^2 \ll |\tilde{x}| \ll 1$.

We now examine the neighbourhood of the singularity, i.e. the inner region. Let us expand the velocity potential at the surface about the current set-down, which is at the constant height ζ_0,

$$\phi|_{z=\zeta} = \left[\phi + \tilde{x}\zeta_1 \frac{\partial \phi}{\partial z} + O(\tilde{x}^2)\right]_{z=\zeta_0}. \tag{5.11}$$

Once again, horizontal derivatives of ϕ must be taken before the expansion, which should not be differentiated with respect to $\tilde{x}$. The kinematic and dynamic surface conditions (3.14) and (3.15) become

$$\frac{\partial \eta}{\partial t} + U_0 \frac{\partial \eta}{\partial x} + \tilde{x} U_1 \frac{\partial \eta}{\partial x} - \frac{\partial \phi}{\partial z} - \tilde{x}\zeta_1 \frac{\partial^2 \phi}{\partial z^2} = O(\epsilon^2, \tilde{x}^2), \tag{5.12}$$

$$\frac{\partial \phi}{\partial t} + \tilde{x}\zeta_1 \frac{\partial^2 \phi}{\partial t \partial z} + U_0 \frac{\partial \phi}{\partial x} + \tilde{x} U_0 \zeta_1 \frac{\partial^2 \phi}{\partial x \partial z} + \tilde{x} U_1 \frac{\partial \phi}{\partial x} + \eta - \Gamma \frac{\partial^2 \eta}{\partial x^2} = O(\epsilon^2, \tilde{x}^2). \tag{5.13}$$

In the neighbourhood of a simple turning point, i.e. the inner region, we expect the spatial dependence of the amplitude to be governed by an Airy differential equation of the form

$$\epsilon^4 \frac{\partial^2 B}{\partial \tilde{x}^2} - c\tilde{x}B = 0. \tag{5.14}$$

The boundary-layer thickness must then be $\tilde{x} = O(\epsilon^{\frac{4}{3}})$. The local characteristic timescale for this inner region is the time for energy to pass through at the propagation speed $c_g + U \sim \tilde{x}^{\frac{1}{2}}$ is

$$t_2 \sim \int_0^{\epsilon^{\frac{4}{3}}} \frac{\mathrm{d}\tilde{x}}{c_g + U} \sim O(\epsilon^{\frac{8}{3}}). \tag{5.15}$$

If transients are important in this inner region, the space and time coordinates for the inner problem must be renormalized by

$$\xi = \epsilon^{-\frac{4}{3}}\tilde{x} \quad \text{and} \quad \tau = \epsilon^{-\frac{2}{3}}t_2, \tag{5.16a, b}$$

which is adopted here for generality. The governing equations (3.5)–(3.8) can be rewritten as follows:

$$\epsilon^{\frac{4}{3}}\frac{\partial^2\phi}{\partial\xi^2}+\frac{\partial^2\phi}{\partial z^2}=0 \quad \text{for} \quad -\infty < z < \zeta_0, \tag{5.17}$$

$$\frac{\partial\phi}{\partial z}=0 \quad \text{for} \quad z\to-\infty, \tag{5.18}$$

$$\epsilon^{\frac{4}{3}}\frac{\partial\eta}{\partial\tau}+\epsilon^{\frac{3}{3}}U_0\frac{\partial\eta}{\partial\xi}+\epsilon^2\xi U_1\frac{\partial\eta}{\partial\xi}-\frac{\partial\phi}{\partial z}-\epsilon^{\frac{4}{3}}\xi\zeta_1\frac{\partial^2\phi}{\partial z^2}=\text{h.o.t.} \quad \text{at} \quad z=\zeta_0, \tag{5.19}$$

$$\epsilon^{\frac{4}{3}}\frac{\partial\phi}{\partial\tau}+\epsilon^{\frac{5}{3}}\xi\zeta_1\frac{\partial^2\phi}{\partial\tau\,\partial z}+\epsilon^{\frac{3}{3}}U_0\frac{\partial\phi}{\partial\xi}+\epsilon^2\xi U_0\zeta_1\frac{\partial^2\phi}{\partial\xi\,\partial z}+\epsilon^2\xi U_1\frac{\partial\phi}{\partial\xi}+\eta-\epsilon^{\frac{4}{3}}\Gamma\frac{\partial^2\eta}{\partial\xi^2}=\text{h.o.t.} \quad \text{at} \quad z=\zeta_0. \tag{5.20}$$

Higher powers in ξ have been incorporated in h.o.t.

Let us assume a solution of the WKB-type

$$\left.\begin{aligned}\phi &= (A+\epsilon^{\frac{2}{3}}A_1+\epsilon^{\frac{4}{3}}A_2+\ldots)\exp\{\mathrm{i}(\epsilon^{-\frac{2}{3}}K_0\xi-\epsilon^{-\frac{4}{3}}\tau)\}+\text{c.c.},\\ \eta &= (B+\epsilon^{\frac{2}{3}}B_1+\epsilon^{\frac{4}{3}}B_2+\ldots)\exp\{\mathrm{i}(\epsilon^{-\frac{2}{3}}K_0\xi-\epsilon^{-\frac{4}{3}}\tau)\}+\text{c.c.}\end{aligned}\right\} \tag{5.21}$$

The lowest-order problem, $O(1)$, is governed by

$$\partial^2A/\partial z^2-K_0^2A=0 \quad \text{for} \quad -\infty < z < \zeta_0, \tag{5.22}$$

$$\partial A/\partial z\to 0 \quad \text{at} \quad z\to-\infty, \tag{5.23}$$

$$-\mathrm{i}B+\mathrm{i}K_0U_0B-\partial A/\partial z=0 \quad \text{at} \quad z=\zeta_0, \tag{5.24}$$

$$-\mathrm{i}A+\mathrm{i}K_0U_0A+B+\Gamma K_0^2B=0 \quad \text{at} \quad z=\zeta_0. \tag{5.25}$$

We shall take as the solution

$$A=-\frac{\mathrm{i}\sigma_0}{K_0}B\,\mathrm{e}^{K_0(z-\zeta_0)} \quad \text{with} \quad B=B(\xi,\tau) \tag{5.26}$$

subject to the dispersion relation

$$1-K_0U_0=(K_0+\Gamma K_0^3)^{\frac{1}{2}}. \tag{5.27}$$

The problem at $O(\epsilon^{\frac{2}{3}})$ is

$$\partial^2A_1/\partial z^2-K_0^2A_1=-2\mathrm{i}K_0\partial A/\partial\xi \quad \text{for} \quad -\infty < z < \zeta_0, \tag{5.28}$$

$$\partial A_1/\partial z=0 \quad \text{at} \quad z\to-\infty, \tag{5.29}$$

$$-\mathrm{i}B_1+U_0\partial B/\partial\xi+\mathrm{i}K_0U_0B_1-\partial A_1/\partial z=0 \quad \text{at} \quad z=\zeta_0, \tag{5.30}$$

$$-\mathrm{i}A_1+U_0\frac{\partial A}{\partial\xi}+\mathrm{i}K_0U_0A_1+B_1-2\mathrm{i}\Gamma K_0\frac{\partial B}{\partial\xi}+\Gamma K_0^2B_1=0 \quad \text{at} \quad z=\zeta_0. \tag{5.31}$$

The last two equations can be combined by eliminating B_1, and the lowest-order result can further be used to substitute for A. The resulting surface condition is

$$\frac{\partial A_1}{\partial z}-K_0A_1=-\frac{\sigma_0}{K_0}\frac{\partial B}{\partial\xi}. \tag{5.32}$$

In obtaining the last result, use has been made of the fact that at the reflection point, $c_g + U_0 = 0$.

The problem for A_1 is seen to be an inhomogeneous version of the homogeneous problem for A. However, it is readily seen that the solvability condition is identically satisfied. We must therefore go to the next order to find a governing equation for A. Particular solutions for A_1 and B_1 can be found as

$$A_1 = -\frac{\sigma_0}{K_0}\frac{\partial B}{\partial \xi}(z-\zeta_0)\,e^{K_0(z-\zeta_0)} \tag{5.33}$$

and

$$B_1 = -i\left(\frac{1}{K_0}+\frac{U_0}{\sigma_0}\right)\frac{\partial B}{\partial \xi}. \tag{5.34}$$

The problem at $O(\epsilon^{\frac{3}{2}})$ is

$$\frac{\partial^2 A_2}{\partial z^2} - K_0^2 A_2 = -\frac{\partial^2 A}{\partial \xi^2} - 2iK_0\frac{\partial A_1}{\partial \xi} \quad \text{for} \quad -\infty < z < \zeta_0, \tag{5.35}$$

$$\partial A_2/\partial z = 0 \quad \text{at} \quad z \to -\infty, \tag{5.36}$$

$$\frac{\partial B}{\partial \tau} - iB_2 + U_0\frac{\partial B_1}{\partial \xi} + iK_0 U_0 B_2 + i\xi K_0 U_1 B - \frac{\partial A_2}{\partial z} - \xi\zeta_1\frac{\partial^2 A}{\partial z^2} = 0 \quad \text{at} \quad z = \zeta_0, \tag{5.37}$$

$$\frac{\partial A}{\partial \tau} - iA_2 - i\xi\zeta_1\frac{\partial A}{\partial z} + U_0\frac{\partial A_1}{\partial \xi} + iK_0 U_0 A_2 + i\xi K_0 U_0\zeta_1\frac{\partial A}{\partial z}$$

$$+ i\xi K_0 U_1 A + B_2 - \Gamma\frac{\partial^2 B}{\partial \xi^2} - 2i\Gamma K_0\frac{\partial B_1}{\partial \xi} + \Gamma K_0^2 B_2 = 0 \quad \text{at} \quad z = \zeta_0. \tag{5.38}$$

The last two equations can be combined by eliminating B_2, and the previous lower-order results can further be used to substitute for A_1, B_1 and A. The resulting surface condition is

$$\frac{\partial A_2}{\partial z} - K_0 A_2 = 2\frac{\partial B}{\partial \tau} - \frac{i}{\sigma_0}[3\Gamma K_0 - U_0^2]\frac{\partial^2 B}{\partial \xi^2} + 2iK_0 U_1 \xi B. \tag{5.39}$$

Both the dispersion relation (5.27) and the identity $c_g = -U_0$ have been used.

The solvability condition for A_2 requires that the right-hand side of (5.39) vanishes, hence B must satisfy the following Schrödinger equation:

$$-i\frac{\partial B}{\partial \tau} - \frac{3\Gamma K_0 - U_0^2}{2\sigma_0}\frac{\partial^2 B}{\partial \xi^2} + K_0 U_1 \xi B = 0. \tag{5.40}$$

Equation (5.40) applies to problems where transients are important in the boundary layer.

For a slowly modulated incident wavepacket, described near the end of §4, the timescale of interest is $t_2 = O(1)$ which is much longer than that of the characteristic time of the inner region defined by (5.16*b*). It is seen that if the modulation timescale is t_2 in (5.40), the inner region is approximately quasi-stationary. Consequently, (5.40) reduces to the ordinary Airy differential equation

$$\partial^2 B/\partial \xi^2 + \alpha^2 \xi B = 0, \tag{5.41}$$

where the coefficient α is defined by (5.7).

The wave amplitude near the reflection point is

$$B(\xi, t_2) = b_0(t_2)\,\mathrm{Ai}(-\alpha^{\frac{2}{3}}\xi), \tag{5.42}$$

where $b_0(t_2)$ remains to be found. As $\alpha^{\frac{2}{3}}\xi \sim \infty$, i.e. far away from the reflection point on the incidence side, the asymptotic behaviour is

$$B \sim b_0(t_2)[\pi^{-\frac{1}{2}}|\alpha|^{-\frac{1}{6}}|\xi|^{-\frac{1}{4}}\sin(\tfrac{2}{3}|\alpha\xi^{\frac{3}{2}}| + \tfrac{1}{4}\pi) + O(\xi^{-\frac{7}{4}})], \tag{5.43}$$

and from (5.34), $$B_1 \sim O(\xi^{\frac{1}{4}}). \tag{5.44}$$

The corresponding asymptotic behaviour of the surface displacement, here expressed in terms of $\tilde{x}$, is

$$\eta(\tilde{x}, t_2) \sim b_0(t_2)\,\pi^{-\frac{1}{2}}|\alpha|^{-\frac{1}{6}}\epsilon^{\frac{1}{3}}|\tilde{x}|^{-\frac{1}{4}}\sin(\tfrac{2}{3}\epsilon^{-2}|\alpha\tilde{x}^{\frac{3}{2}}| + \tfrac{1}{4}\pi)\exp(\mathrm{i}\epsilon^{-2}[K_0\tilde{x} - t_2]). \tag{5.45}$$

This is the outer expansion of the inner solution.

Higher powers of $\tilde{x}$ from B give contributions of $O(\epsilon^{\frac{7}{3}}\tilde{x}^{-\frac{7}{4}})$, while terms from B_1 give contributions of $O(\epsilon^{\frac{1}{3}}\tilde{x}^{\frac{1}{4}})$. Therefore, this one-term asymptotic expansion is valid in the region $\epsilon^{\frac{4}{3}} \ll |\tilde{x}| \ll 1$.

Both asymptotic expansions (5.10) and (5.45) have a common region of validity, $\epsilon^{\frac{4}{3}} \ll |\tilde{x}| \ll 1$. The relationship between the coefficients can now be found by asymptotic matching. The time-dependent coefficients of the ray solution, (5.10), are most easily evaluated at the time when the ray reaches the reflection point. Hence the time integrals in (5.10) are to be evaluated with the upper limit set to $\tilde{x} = 0$. This can be done because the errors introduced in the time and phase integrals are smaller than the accuracy of the asymptotic result. The results of matching are then

$$b_+\left(t_2 - \int_{\tilde{x}_+}^{0} \frac{\mathrm{d}\tilde{x}}{c_{\mathrm{g}}^{+} + U}\right) = -\mathrm{i}b_-\left(t_2 - \int_{\tilde{x}_-}^{0} \frac{\mathrm{d}\tilde{x}}{c_{\mathrm{g}}^{-} + U}\right)\exp\left\{\mathrm{i}\epsilon^{-2}\left[\int_{\tilde{x}_-}^{0} K^-\,\mathrm{d}\tilde{x} - \int_{\tilde{x}_+}^{0} K^+\,\mathrm{d}\tilde{x}\right]\right\}, \tag{5.46}$$

and

$$b_0(t_2) = b_-\left(t_2 - \int_{\tilde{x}_-}^{0} \frac{\mathrm{d}\tilde{x}}{c_{\mathrm{g}}^{-} + U}\right)\epsilon^{-\frac{1}{3}}\left|\frac{2\pi}{\sigma_0 U_1}\right|^{\frac{1}{2}}|\alpha|^{\frac{2}{3}}\exp\left(\mathrm{i}\epsilon^{-2}\int_{\tilde{x}_-}^{0} K^-\,\mathrm{d}\tilde{x} - \tfrac{1}{4}\pi\mathrm{i}\right). \tag{5.47}$$

Both the inner and outer solutions are therefore determined. The theory is equally valid in either of regions IV and V in figure 5, by a proper choice of solution branches of the dispersion relation.

To summarize, the amplitude far from the reflection point is given by (5.10) while the solution at the reflection point is given by (5.42). A solution uniformly valid to the leading order with $O(\epsilon^{\frac{2}{3}})$ error can be obtained by adding the inner and outer solutions and subtracting the common asymptotic part in (5.45).

Numerical examples will be discussed in §8.

We remark that improved results including $\epsilon^{\frac{2}{3}}(A_1, B_1)$ may be pursued in principle. On the other hand, by keeping just the leading order in the outer ray approximation, the error is $O(\epsilon^2)$ which is relatively small.

6. Solution near a perfect triple turning point

As shown in figure 4, for a sufficiently low wave frequency, there are two simple reflection points (double-roots of (4.14*b*)). For a sufficiently high frequency, there are no reflection points. Therefore, a triple-root point exists for some intermediate wave frequency, ω_0, where the two reflection points coalesce. We now assume the incident wave frequency to be precisely the critical frequency $\bar{\omega} = \omega_0$.

From (4.14*a*, *b*), the following three conditions must be satisfied simultaneously at the perfect triple-root point: the dispersion relation

$$\Gamma_0 K_0^3 - U_0^2 K_0^2 + (2U_0 + 1) K_0 - 1 = 0; \tag{6.1}$$

the condition for a reflection point $\mathrm{d}\sigma/\mathrm{d}K = -U$

$$3\Gamma_0 K_0^2 - 2U_0^2 K_0 + 2U_0 + 1 = 0; \tag{6.2}$$

and the condition for a triple-root $\mathrm{d}^2\sigma/\mathrm{d}K^2 = 0$

$$3\Gamma_0 K_0 - U_0^2 = 0. \tag{6.3}$$

We have denoted the critical solution at the triple-root point by subscript zero. The solution to (6.1)–(6.3) is

$$K_0 = 3 + 2\sqrt{3}, \quad \Gamma_0 = -5 + \tfrac{26}{9}\sqrt{3}, \quad U_0 = -2 + \sqrt{3}, \quad \sigma_0 = 1 + \sqrt{3}. \tag{6.4}$$

Recall that the dimensionless quantities (in capital letters K_0, U_0, Γ_0) are related to the dimensional quantities (in small letters k_0, u_0, ω_0) by $\Gamma_0 = T\omega_0^4/(\rho g^3)$, $K_0 = gk_0/\omega_0^2$ and $U_0 = \omega_0 u_0/g$. For typical values $g = 9.8\ \mathrm{m/s^2}$ and $T/\rho = 7.3 \times 10^{-5}\ \mathrm{m^3/s^2}$, the triple point occurs when the absolute frequency is 2.4 Hz, the wavelength is 4.4 cm and the current velocity is -18 cm/s.

Let us define the local, slow horizontal coordinate as $\tilde{x} = x_2 - x_0$, where x_0 is the location of the triple turning point. Let the current field be expanded as in §5,

$$\left.\begin{aligned} \zeta &= \zeta_0 + \tilde{x}\zeta_1 + O(\tilde{x}^2), \\ U &= U_0 + \tilde{x}U_1 + O(\tilde{x}^2, \epsilon^3\tilde{x}). \end{aligned}\right\} \tag{6.5}$$

To find the asymptotic behaviour of the wavenumber, we substitute the surface current expansion (6.5) and the following expansion for the wavenumber,

$$K = K_0 + R(\tilde{x}, \epsilon), \tag{6.6}$$

into the dispersion relation (4.14*b*). The resulting expressions can then be simplified by using the exact solution (6.4).

The equation governing the leading behaviour of the wavenumber is

$$R^3\Gamma_0 + 2U_1 K_0 \sigma_0 \tilde{x} = O(\tilde{x}R), \tag{6.7}$$

which suggests an asymptotic expansion in powers of $\tilde{x}^{\frac{1}{3}}$. We then assume

$$K \sim K_0 + \alpha\tilde{x}^{\frac{1}{3}} + \alpha_2\tilde{x}^{\frac{2}{3}} + \alpha_3\tilde{x}, \tag{6.8}$$

and determine

$$\alpha = \left(-\frac{2K_0\sigma_0 U_1}{\Gamma_0}\right)^{\frac{1}{3}} = [-(4770 + 2754\sqrt{3})\, U_1]^{\frac{1}{3}}, \tag{6.9}$$

$$\alpha_2 = \frac{-21 + 13\sqrt{3}}{18}\alpha^2, \quad \alpha_3 = \frac{33 - 19\sqrt{3}}{18}\alpha^3. \tag{6.10}$$

This expansion is asymptotically valid for $|\tilde{x}| \ll 1$.

Substitution of the expansions for U and K into the ray solution (4.28), gives the behaviour for small $\tilde{x}$, i.e. the inner expansion of the outer ray approximation,

$$B^{(\pm)}(\tilde{x}, t_2) = b_\pm\left(t_2 - \int_{\tilde{x}_\pm}^{\tilde{x}} \frac{\mathrm{d}\tilde{x}}{c_g + U}\right)\left(\frac{K}{\sigma(c_g + U)}\right)^{\frac{1}{2}}$$

$$\sim b_\pm\left(t_2 - \int_{\tilde{x}_\pm}^{\tilde{x}} \frac{\mathrm{d}\tilde{x}}{c_g + U}\right)\left\{\sqrt{6}(7 + 4\sqrt{3})\,\alpha^{-1}|\tilde{x}|^{-\frac{1}{3}} + \frac{\sqrt{2}(5 + 3\sqrt{3})}{12}\,\mathrm{sign}\,(\tilde{x}) + O(\tilde{x}^{\frac{1}{3}})\right\}. \tag{6.11}$$

As before, we let indices $-$ and $+$ denote the longer incident wave from $\tilde{x} < 0$ and the shorter transmitted wave to $\tilde{x} > 0$, respectively. We also let $\tilde{x}_\pm$ be the starting points for the time and phase integrals on either side.

From the inhomogeneous Laplace equation at $O(\epsilon^2)$, (4.16), the dominant $\tilde{x}$-behaviour of $B_2^\pm$ near $\tilde{x} = 0$ is

$$A_2^\pm \sim B_2^\pm \sim O(\tilde{x}^{-\frac{1}{2}}). \tag{6.12}$$

Therefore, the surface displacement on either side of the singularity can be expanded as

$$\begin{aligned}\eta^{(\pm)}(\tilde{x}, t_2) &= (B^{(\pm)} + \epsilon^2 B_2^{(\pm)} + \ldots)\exp\left\{\mathrm{i}\epsilon^{-2}\left[\int_{x_\pm}^{\tilde{x}} K\,\mathrm{d}\tilde{x} - t_2\right]\right\} + \text{c.c.} \\ &\sim b_\pm\left(t_2 - \int_{\tilde{x}_\pm}^{\tilde{x}} \frac{\mathrm{d}\tilde{x}}{c_g + U}\right)\left\{\sqrt{6(7+4\sqrt{3})}\,\alpha^{-1}|\tilde{x}|^{-\frac{1}{2}} + \frac{\sqrt{2(5+3\sqrt{3})}}{12}\operatorname{sign}(\tilde{x})\right\} \\ &\quad \times \exp\left\{\mathrm{i}\epsilon^{-2}\left[\int_{\tilde{x}_\pm}^{0} K\,\mathrm{d}\tilde{x} + K_0\tilde{x} + \tfrac{3}{4}\alpha\tilde{x}^{\frac{4}{3}} - t_2\right]\right\} + \text{c.c.}\end{aligned} \tag{6.13}$$

In this outer approximation, the singularity is more severe than for a simple reflection point. Moreover, the second term of the expansion (6.13) is non-vanishing as $\tilde{x} \to 0$. Therefore, a satisfactory theory for the triple turning point will require at least a two-term expansion, so that the truncation error is asymptotically vanishing.

In this case of a perfect triple root, it can be shown that the two-term inner expansion of the outer ray approximation is valid for $\epsilon^{\frac{3}{2}} \ll |\tilde{x}| \ll 1$. The one-term expansion is valid for a much larger region $\epsilon^2 \ll |\tilde{x}| \ll 1$.

We next proceed to find the inner solution in the neighbourhood of the triple turning point, $\tilde{x} = 0$. An envelope equation is anticipated of the form

$$\epsilon^6 \partial^3 B/\partial\tilde{x}^3 + c\tilde{x}B = 0; \tag{6.14}$$

the corresponding boundary-layer thickness is $\tilde{x} = O(\epsilon^{\frac{3}{2}})$. Asymptotic evaluation of the energy propagation speed for the ray solution now gives $c_g + U \sim \tilde{x}^{\frac{3}{2}}$. Therefore, a characteristic time for energy to propagate through the inner region is

$$t_2 \sim \int_0^{\epsilon^{\frac{3}{2}}} \frac{\mathrm{d}\tilde{x}}{c_g + U} \sim O(\epsilon^{\frac{1}{2}}). \tag{6.15}$$

If transients are allowed in the inner region, the following boundary-layer coordinates are appropriate:

$$\xi = \epsilon^{-\frac{3}{2}}\tilde{x} \quad \text{and} \quad \tau = \epsilon^{-\frac{1}{2}}t_2. \tag{6.16a, b}$$

The governing equations (3.5)–(3.8) can be rewritten as follows:

$$\epsilon\,\partial^2\phi/\partial\xi^2 + \partial^2\phi/\partial z^2 = 0 \quad \text{for} \quad -\infty < z < \zeta_0, \tag{6.17}$$

$$\partial\phi/\partial z = 0 \quad \text{for} \quad z \to -\infty, \tag{6.18}$$

$$\epsilon^{\frac{3}{2}}\frac{\partial\eta}{\partial\tau} + \epsilon^{\frac{1}{2}}U_0\frac{\partial\eta}{\partial\xi} + \epsilon^2 U_1\xi\frac{\partial\eta}{\partial\xi} - \frac{\partial\phi}{\partial z} - \epsilon^{\frac{3}{2}}\zeta_1\xi\frac{\partial^2\phi}{\partial z^2} = \text{h.o.t.} \quad \text{at} \quad z = \zeta_0, \tag{6.19}$$

$$\epsilon^{\frac{3}{2}}\frac{\partial\phi}{\partial\tau} + \epsilon^3\zeta_1\xi\frac{\partial^2\phi}{\partial\tau\,\partial z} + \eta + \epsilon^{\frac{1}{2}}U_0\frac{\partial\phi}{\partial\xi} + \epsilon^2 U_0\zeta_1\xi\frac{\partial^2\phi}{\partial\xi\,\partial z} + \epsilon^2 U_1\xi\frac{\partial\phi}{\partial\xi} - \epsilon\Gamma_0\frac{\partial^2\eta}{\partial\xi^2} = \text{h.o.t.}$$

$$\text{at} \quad z = \zeta_0. \tag{6.20}$$

The following WKB expansions are assumed:

$$\left.\begin{aligned}\phi &= (A+\epsilon^{\frac{1}{2}}A_1+\epsilon A_2+\epsilon^{\frac{3}{2}}A_3+\ldots)\exp\{\mathrm{i}(\epsilon^{-\frac{1}{2}}K_0\xi-\epsilon^{-\frac{3}{2}}\tau\}+\text{c.c.},\\ \eta &= (B+\epsilon^{\frac{1}{2}}B_1+\epsilon B_2+\epsilon^{\frac{3}{2}}B_3+\ldots)\exp\{\mathrm{i}(\epsilon^{-\frac{1}{2}}K_0\xi-\epsilon^{-\frac{3}{2}}\tau\}+\text{c.c.}\end{aligned}\right\} \tag{6.21}$$

The problems at $O(1)$ and $O(\epsilon^{\frac{1}{2}})$ are identical to the case of a simple reflection point, and therefore the solutions (5.26), (5.33) and (5.34) still hold.

The $O(\epsilon)$ problem is

$$\frac{\partial^2 A_2}{\partial z^2}-K_0^2 A_2 = -\frac{\partial^2 A}{\partial \xi^2}-2\mathrm{i}K_0\frac{\partial A_1}{\partial \xi} \quad \text{for} \quad -\infty < z < \zeta_0, \tag{6.22}$$

$$\partial A_2/\partial z = 0 \quad \text{at} \quad z\to-\infty, \tag{6.23}$$

$$-\mathrm{i}\sigma_0 B_2+U_0\,\partial B_1/\partial\xi-\partial A_2/\partial z = 0 \quad \text{at} \quad z=\zeta_0, \tag{6.24}$$

$$-\mathrm{i}\sigma_0 A_2+U_0\frac{\partial A_1}{\partial\xi}+B_2-\Gamma_0\frac{\partial^2 B}{\partial\xi^2}-2\mathrm{i}\Gamma_0 K_0\frac{\partial B_1}{\partial\xi}+\Gamma_0 K_0^2 B_2 = 0 \quad \text{at} \quad z=\zeta_0. \tag{6.25}$$

The last two equations can be combined to eliminate B_2, and the lower-order results can further be used to eliminate A, A_1 and B_1. Making use of the exact values of K_0, Γ_0, U_0 and σ_0, we arrive at the following surface condition:

$$\partial A_2/\partial z - K_0 A_2 = 0. \tag{6.26}$$

The solvability condition can again be shown to be identically satisfied. The particular solution at this order can be summarized as

$$A_2 = \frac{\mathrm{i}\sigma_0}{2K_0}(z-\zeta_0)^2\frac{\partial^2 B}{\partial\xi^2}\mathrm{e}^{K_0(z-\zeta_0)}, \tag{6.27}$$

$$B_2 = -\left(\frac{U_0}{K_0\sigma_0}+\frac{U_0^2}{\sigma_0^2}\right)\frac{\partial^2 B}{\partial\xi^2}. \tag{6.28}$$

The problem at $O(\epsilon^{\frac{3}{2}})$ is

$$\frac{\partial^2 A_3}{\partial z^2}-K_0^2 A_3 = -\frac{\partial^2 A_1}{\partial\xi^2}-2\mathrm{i}K_0\frac{\partial A_2}{\partial\xi} \quad \text{for} \quad -\infty < z < \zeta_0, \tag{6.29}$$

$$\partial A_3/\partial z = 0 \quad \text{at} \quad z\to-\infty, \tag{6.30}$$

$$\frac{\partial B}{\partial\tau}-\mathrm{i}\sigma_0 B_3+U_0\frac{\partial B_2}{\partial\xi}+\mathrm{i}K_0 U_1\xi B-\frac{\partial A_3}{\partial z}-\zeta_1\xi\frac{\partial^2 A}{\partial z^2} = 0 \quad \text{at} \quad z=\zeta_0, \tag{6.31}$$

$$\frac{\partial A}{\partial\tau}-\mathrm{i}\sigma_0 A_3+U_0\frac{\partial A_2}{\partial\xi}+B_3-\Gamma_0\frac{\partial^2 B_1}{\partial\xi^2}-2\mathrm{i}\Gamma_0 K_0\frac{\partial B_2}{\partial\xi}$$

$$+\Gamma_0 K_0^2 B_3+\mathrm{i}K_0 U_1\xi A-\mathrm{i}\sigma_0\zeta_1\xi\frac{\partial A}{\partial z} = 0 \quad \text{at} \quad z=\zeta_0. \tag{6.32}$$

If the last two equations are combined to eliminate B_3, and the lower-order results are used to eliminate A, A_1, A_2, B_1 and B_2, we get the surface condition

$$\frac{\partial A_3}{\partial z}-K_0 A_3 = 2\frac{\partial B}{\partial\tau}-\frac{\Gamma_0}{\sigma_0}\frac{\partial^3 B}{\partial\xi^3}+2\mathrm{i}K_0 U_1\xi B. \tag{6.33}$$

The solvability condition gives the following third-order partial differential equation governing the complex envelope B,

$$\frac{\partial B}{\partial \tau} - \frac{\Gamma_0}{2\sigma_0}\frac{\partial^3 B}{\partial \xi^3} + \mathrm{i}K_0 U_1 \xi B = 0. \tag{6.34}$$

Employing the theory of averaged Lagrangian and including nonlinearities, Peregrine & Smith (1979) deduced formally a similar equation with a cubic nonlinearity. However, they did not work out the coefficients explicitly, and hence did not examine the physical implications in detail.

For a slowly modulated incident wavepacket, described near the end of §4, the timescale of interest is $t_2 = O(1)$, which is much longer than that of the characteristic time of the inner region defined by (6.16*b*). It is seen that if the modulation timescale is t_2 in (6.34), the inner region is approximately *quasi*-stationary. Consequently, the stationary limit of (6.34) reduces to the following Pearcey differential equation for the amplitude B:

$$\frac{\partial^3 B}{\partial \xi^3} - \frac{2\mathrm{i}K_0\sigma_0 U_1}{\Gamma_0}\xi B = 0. \tag{6.35}$$

The solution of this equation is a special case of the Pearcey function. With reference to Appendix A, the solution which is bounded as $\xi \to \pm\infty$ is

$$B(\xi, t_2) = b_0(t_2) P(Y), \tag{6.36}$$

where $P(Y)$ denotes the Pearcey function defined by (A 5). Here, Y is the complex argument

$$Y = \sqrt{2}\alpha^{\frac{3}{4}} \mathrm{e}^{-\pi\mathrm{i}/8}\xi, \tag{6.37}$$

and α is the coefficient in the wavenumber expansion (6.9). For convenience, we give in Appendix A approximations for large ξ, which can be found in Paris (1991).

The solutions for B_1 and B_2 are now given by

$$\begin{aligned} B_1 &= -\mathrm{i}\left[\frac{1}{K_0} + \frac{U_0}{\sigma_0}\right]\frac{\partial B}{\partial \xi} + \text{homogeneous solution} \\ &= \mathrm{i}b_0(t_2)\left[\frac{1}{K_0} + \frac{U_0}{\sigma_0}\right]\sqrt{2}\alpha^{\frac{3}{4}}\mathrm{e}^{-\pi\mathrm{i}/8}\frac{\partial P(Y)}{\partial Y} + b_1(t_2) P(Y) \end{aligned} \tag{6.38}$$

and

$$B_2(\xi, t_2) \sim \partial^2 P(Y)/\partial Y^2 \sim O(\xi^{\frac{1}{2}}), \tag{6.39}$$

cf. (5.34) and (6.28). To simplify the notation, we shall recombine the arbitrary complex constants as follows:

$$c_0 = b_0 + \epsilon^{\frac{1}{2}} b_1 \quad \text{and} \quad c_1 = -\mathrm{i}b_0\left[\frac{1}{K_0} + \frac{U_0}{\sigma_0}\right]\sqrt{2}\alpha^{\frac{3}{4}}\mathrm{e}^{-\pi\mathrm{i}/8}, \tag{6.40}$$

which must be determined by asymptotic matching. Afterwards, the surface displacement η becomes

$$\begin{aligned} \eta(\xi, t_2) &= [B + \epsilon^{\frac{1}{2}} B_1 + \epsilon B_2 + \ldots]\mathrm{e}^{\mathrm{i}\epsilon^{-\frac{1}{2}}K_0\xi - \mathrm{i}t} + \text{c.c.} \\ &\sim \left[c_0(t_2) P(Y) + \epsilon^{\frac{1}{2}} c_1(t_2)\frac{\partial P(Y)}{\partial Y} + O(\epsilon\xi^{\frac{1}{2}})\right]\mathrm{e}^{\mathrm{i}\epsilon^{-\frac{1}{2}}K_0\xi - \mathrm{i}t} + \text{c.c.} \end{aligned} \tag{6.41}$$

We now need the large-argument expansion ($\xi \to \pm\infty$) of the inner surface displacement approximation. With reference to Appendix A, we note that for $|\arg Y| < \frac{3}{8}\pi$, the Pearcey function take the form

$$P(Y) = P_0(Y) + P_1(Y), \tag{6.42}$$

where P_0 is algebraically decaying in ξ and P_1 is exponentially decaying in ξ. Hence for purposes of asymptotic matching, we need only consider P_0, whose large-ξ expansion is

$$P_0(Y) \sim (\tfrac{1}{3}\pi)^{\frac{1}{2}} e^{-\pi i/8} \exp(\tfrac{3}{4}i\alpha\xi^{\frac{4}{3}}) \{\alpha^{-\frac{1}{4}}|\xi|^{-\frac{1}{3}} + O(\xi^{-\frac{5}{3}})\}. \tag{6.43}$$

Correspondingly, the asymptotic behaviour for η, here expressed in terms of the outer variable $\tilde{x}$, is

$$\eta(\tilde{x}, t_2) \sim [c_0(t_2)(\tfrac{1}{3}\pi\epsilon)^{\frac{1}{2}} e^{-\pi i/8}\alpha^{-\frac{1}{4}}|\tilde{x}|^{-\frac{1}{3}} + c_1(t_2)(\tfrac{1}{6}\pi\epsilon)^{\frac{1}{2}} i \operatorname{sign}(\tilde{x}) + O(\epsilon^{\frac{1}{2}}\tilde{x}^{\frac{1}{3}})] \times \exp\{i\epsilon^{-2}(K_0\tilde{x} + \tfrac{3}{4}\alpha\tilde{x}^{\frac{4}{3}})\}. \tag{6.44}$$

When this outer expansion of the inner solution is compared with the inner expansion of the outer solution (6.13), it is clear that both the amplitude and the phase match to two significant terms.

From (6.43) we see that higher-order terms from B are $O(\epsilon^{\frac{5}{2}}\tilde{x}^{-\frac{5}{3}})$, higher-order terms from B_1 are $O(\epsilon^{\frac{3}{2}}\tilde{x}^{-\frac{4}{3}})$, while terms from B_2 are $O(\epsilon^{\frac{1}{2}}\tilde{x}^{\frac{1}{3}})$. From this it follows that the one-term asymptotic form is valid for $\epsilon^{\frac{3}{2}} \ll |\tilde{x}| \ll 1$, and the two-term asymptotic form is valid for $\epsilon^{\frac{6}{5}} \ll |\tilde{x}| \ll 1$.

The inner and outer solutions have an overlapping region of validity for their respective asymptotic expansions. The matching region for a one-term match is $\epsilon^{\frac{3}{2}} \ll |\tilde{x}| \ll 1$, and for a two-term match is $\epsilon^{\frac{6}{5}} \ll |\tilde{x}| \ll 1$. Higher-order asymptotic matching is seen to give a smaller matching region, as is usually expected.

Similarly to the case of a simple reflection point, we fix the time-dependent coefficients of the ray solution, (6.13), at the time when the ray reaches the triple-root point. We can do this because the relative error introduced is small, less than the accuracy of the asymptotic match. Hence the time and phase integrals in equation (6.13) are to be evaluated with the upper limit set to $\tilde{x} = 0$. Asymptotic matching now gives $c_0(t_2)$, $c_1(t_2)$ and $b_+(t_2)$ in terms of the incident wave $b_-(t_2)$ as follows

$$c_0(t_2) = b_-\left(t_2 - \int_{\tilde{x}_-}^{0} \frac{d\tilde{x}}{c_g + U}\right) \frac{\sqrt{2(21+12\sqrt{3})}}{(\pi\epsilon)^{\frac{1}{2}}} \alpha^{-\frac{3}{4}} \exp\left\{i\epsilon^{-2}\int_{\tilde{x}_-}^{0} K\,d\tilde{x} + \frac{\pi i}{8}\right\}, \tag{6.45}$$

$$c_1(t_2) = b_-\left(t_2 - \int_{\tilde{x}_-}^{0} \frac{d\tilde{x}}{c_g + U}\right) \frac{9+5\sqrt{3}}{6(\pi\epsilon)^{\frac{1}{2}}} \exp\left\{i\epsilon^{-2}\int_{\tilde{x}_-}^{0} K\,d\tilde{x} - \frac{\pi i}{2}\right\} \tag{6.46}$$

and

$$b_+\left(t_2 - \int_{\tilde{x}_+}^{0} \frac{d\tilde{x}}{c_g + U}\right) = b_-\left(t_2 - \int_{\tilde{x}_-}^{0} \frac{d\tilde{x}}{c_g + U}\right) \exp\left\{i\epsilon^{-2}\int_{\tilde{x}_-}^{\tilde{x}_+} K\,d\tilde{x}\right\}. \tag{6.47}$$

We note that both coefficients for the inner solution have the same order in ϵ; this indicates that the matching is consistent with respect to the ordering parameter.

In summary, the outer solutions in regions I and III, depicted in figure 5, are still given by (6.13), and the inner solution, which now covers all of regions II, IV and V, is given by (6.41) where the coefficients are given by (6.45)–(6.47).

Numerical results will be presented in §8.

The remark at the end of §5 is also appropriate here. For a successful asymptotic matching, we need to consider two terms in the inner approximation (6.21). The relative difference between consecutive terms in (6.21) is only $\epsilon^{\frac{1}{2}}$. To reduce the truncation error at and near the turning point, it would be desirable to include one more term, $A_2, B_2 \propto P''(Y)$. This is a very lengthy task. On the other hand, keeping the leading-order term in the outer approximation implies a much smaller error of $O(\epsilon^2)$.

If the triple-root conditions are not exactly met, a theory that accounts for slight detuning is needed. This theory has been worked out, but the mathematical complexity increases enormously, and is not reported here.

7. Remarks on existing experiments

Pokazeyev & Rozenberg (1983) performed experiments for wavepackets on coflowing and counterflowing currents over a sloping bottom in a wave tank. The wavepackets typically contained 3–10 waves with the central frequency 2–11 Hz. The countercurrent varied from 0.04 m/s at the deep end to 0.2 m/s at the shallow end of a slope of length 0.8 m. From figure (5*c*) in their paper, the current varied linearly with distance along the tank. Most of the cases discussed in their paper are for frequencies too high (> 2.4 Hz) for double reflection. Detailed time series records were not reported; amplitude plots were presented as if the wavetrains were uniform. Only one case, with frequency 2 Hz, corresponds to double reflection. However, for this frequency only one or two amplitude measurements were recorded between the two reflection points, which are separated by 6 cm, as can be estimated from figure 4. This lack of information precludes a meaningful comparison with our theory.

In a subsequent paper, Badulin *et al.* (1983) performed wavepacket experiments for lower frequencies 1.5–3 Hz with a view to observing double reflection. The current velocity varied over the same range, 0.04–0.2 m/s, but now over a slope of length 1.6 m. Amplitude data were presented schematically as a continuous function of the horizontal distance for one frequency only (2 Hz). According to their description, the data were recorded at every 2.5 cm. For the given current gradient, the distance between the reflection points is about 12 cm, which implies that there were 4 or 5 measurements in this region. However, without knowledge of the time and positions of the measurements in the relatively narrow region where modulation is strong, a comparison with our theory cannot be made.

In both experiments, the parameter $\epsilon = (\bar{k}L)^{-\frac{1}{2}}$ is not small. For the two slope lengths, 0.8 and 1.6 m, the current can be estimated at $\partial U/\partial x = 0.2$, 0.1 s^{-1}. Defining the long lengthscale of the current by

$$\frac{1}{L} = \frac{1}{U_{\mathrm{ave}}} \frac{\partial U}{\partial x}, \tag{7.1}$$

where U_{ave} is the average current over the slope, we estimate $L = 0.6$ and 1.2 m, respectively. It follows from (2.3) that for $\omega/2\pi = 2$ Hz, $\epsilon = 0.32$ and 0.23, respectively, which are not small.

Viscous damping is also important in these experiments. Pokazeyev & Rozenberg (1983) measured the amplitude attenuation rates in zero and constant currents, and found the actual damping rate to be 2–3 times that of a semi-theoretical model combining viscous dissipation in the interior of the fluid, boundary-layer dissipation and losses near the free surface which is assumed to be an inextensible film.

For pure gravity waves on a variable current, Lai, Long & Huang (1989) performed

similar experiments by focusing attention on the kinematics only. They confirmed the dispersion relation and the implied reflection, but no measurements on amplitude variations were reported.

Clearly, a meaningful comparison between experiments and theory awaits more detailed measurements of amplitude and proper accounting for damping, detuning and nonlinearity.

8. Numerical results for wavepackets

We now describe the time evolution of wavepackets with two different central frequencies, one lower than and one equal to the frequency for the perfect triple turning point.

For $\omega/2\pi = 1.9$ Hz, far lower than the triple-root frequency (2.4 Hz), there are two reflection points. The distance between them depends on the current gradient, which is chosen to be a constant small enough so that the reflection points are sufficiently far apart to be treated independently of each other.

In all the plots, the peak amplitude at the left edge of the figure is normalized to unity. The locations of the turning points are indicated by vertical lines. In order to suggest possible experiments, the abscissa are labelled by the position in metres.

Case 1. Large separation between two reflection points

Referring to figures 6 and 7, which cover the entire horizontal extent of the sloping bottom, the current velocity at the left edge is -0.19 m/s and at the right edge -0.22 m/s. We assume the current gradient to be constant, $\partial U/\partial x = -0.0075\ \mathrm{s}^{-1}$, over a slope of 4 m length. The length L of normalization should be about $L = 27$ m, calculated according to (7.1). This gives the dimensionless parameters $\epsilon = 0.050$ and $\Gamma = 0.0016$. Recall that the dimensionless parameter ϵ was defined as the ratio of the wavelength of a pure gravity wave of the given frequency on still water, to the current lengthscale L. Since the wavelength in the zone of reflections is always shorter than that of the pure gravity wave, the local ratio between the short and long scales is never larger than the one given above. The boundary condition at the left edge of each snapshot is (in non-dimensional variables)

$$\eta(t_2) = \exp\{-c(t_2 - T)^2 - \mathrm{i}\epsilon^{-2}(t_2 - T)\}, \tag{8.1}$$

where $c = 0.5$. Starting with $T = 0$, the time interval between each snapshot is $\Delta T = 1.2$. Alternatively, in physical coordinates,

$$\eta(t^*) = \exp\{-c^*(t^* - T^*)^2 - \mathrm{i}\omega(t^* - T^*)\}, \tag{8.2}$$

where $c^* \approx 4.5 \times 10^{-4}\ \mathrm{s}^{-2}$ and T^* increases in steps of about 40 s.

To estimate crudely the effect of viscous damping, we introduce in the ray solutions the theoretical value accounting for internal dissipation only. Specifically, we use the model of Shyu & Phillips (1990),

$$\frac{\partial}{\partial t_2}\left(\frac{E}{\sigma}\right) + \frac{\partial}{\partial x_2}\left((c_g + U)\frac{E}{\sigma}\right) = -\chi K^2 \frac{E}{\sigma}, \tag{8.3}$$

where $\chi = 4\epsilon^{-2}\nu\omega^3/g^2$ is a dimensionless parameter. In the present case, the parameter is $\chi = 0.028$.

We first show the development without damping in figure 6. The drastic reduction

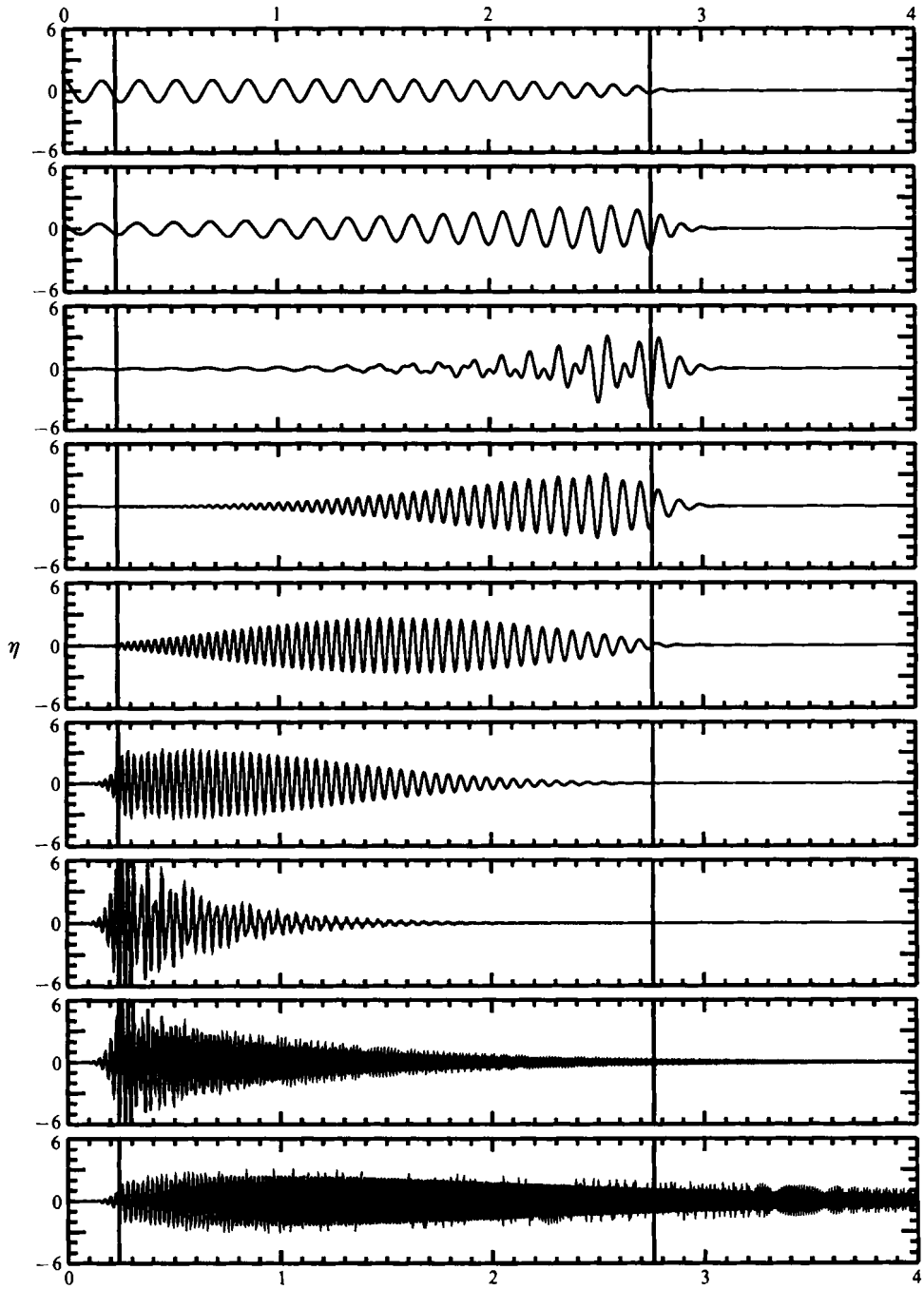

FIGURE 6. Two well separated reflection points with frequency 1.9 Hz, current gradient $-0.0075\ s^{-1}$. No damping. The abscissa shows the position in metres, the ordinate shows normalized amplitude relative to peak unit amplitude at the left edge.

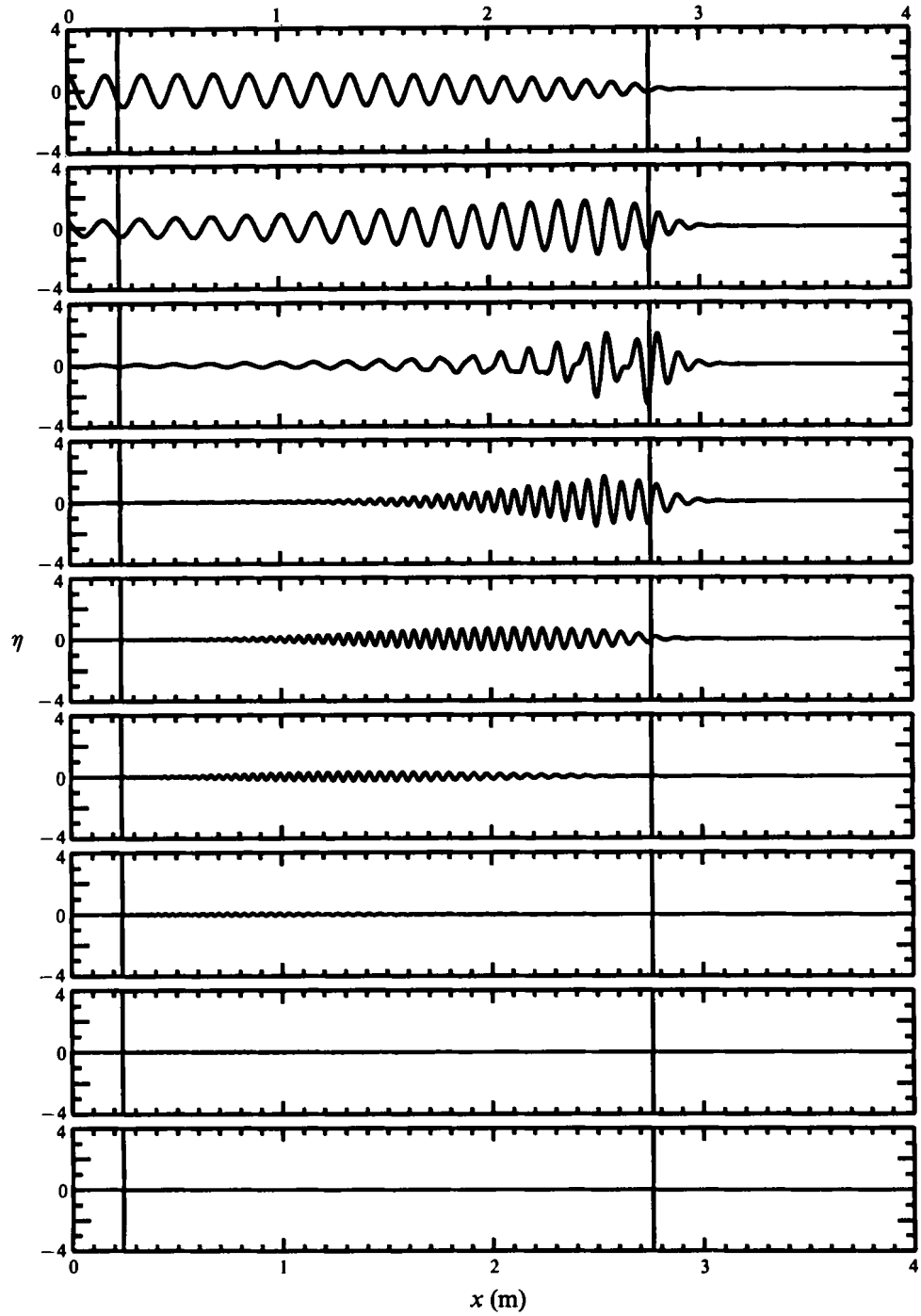

FIGURE 7. Two well separated reflection-points with frequency 1.9 Hz, current gradient $-0.0075\ s^{-1}$. Waves away from the reflection points are damped.

of wavelength after the second reflection is evident. In figure 7 damping is introduced for the ray solutions away from the reflection points. Since the distance between the reflection points is large, the short gravity wave reflected from the first reflection point is completely damped out before it reaches the second reflection point.

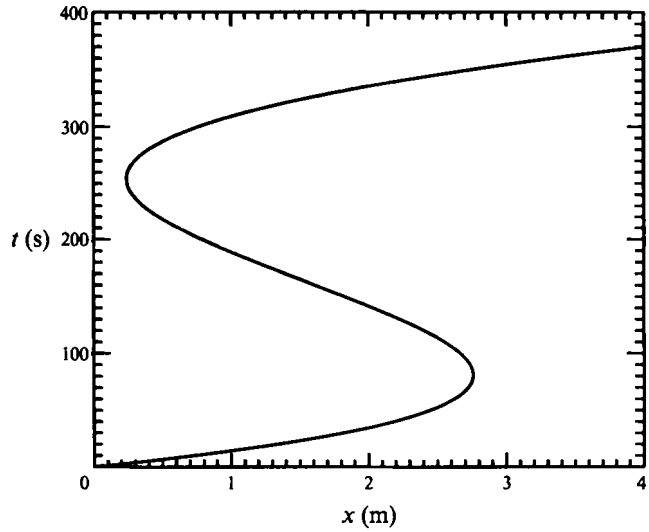

FIGURE 8. The trajectory of the envelope peak for frequency 1.9 Hz and current gradient $-0.0075\ \mathrm{s}^{-1}$. The abscissa shows position in metres, the ordinate shows elapsed time in seconds.

Corresponding to figures 6 and 7, we plot in figure 8 the trajectory of the envelope peak as a function of time, according to the characteristic curve for the ray solution given by (4.27). We have labelled the abscissa in metres in accordance with the other figures, while the ordinate shows the elapsed time in seconds. It is evident that despite the reduction of wavelength the speed of the envelope remains comparable.

If the characteristic time for viscous damping is calculated at the two reflection points as $\tau = 1/(\nu k^2)$, we find $\tau \approx 250$ s at the (first) gravity reflection point and $\tau \approx 18$ s at the (second) capillary reflection point. We now calculate the characteristic time, according to the ray theory, for the centre of the wavepacket to propagate through the inner regions. This is done by measuring on figure 8 the time it takes to pass through the inner region corresponding to setting the inner variable $\xi = O(1)$. Let U_0 and k_0 be the local values for the current and wavenumber at the reflection point. Then $L_0 = U_0/(\partial U/\partial x)$ and $\epsilon_0 = 1/(k_0 L_0)^{\frac{1}{2}}$ are the local values for the long lengthscale and the ordering parameter. According to (5.16), the thickness of the inner region should then be $\Delta x = 1/(\epsilon_0^{\frac{5}{3}} k_0) = k_0^{-\frac{8}{3}} L_0^{\frac{1}{3}}$. The characteristic times of propagation through the inner regions should therefore be 55 s at the gravity reflection point and 35 s at the capillary reflection point. Hence damping in the inner region of the gravity reflection point should be negligible as assumed, but considerable at the capillary reflection point. In this case, however, the capillary wave is completely damped out before it reaches the capillary reflection point, the error introduced by not accounting for dissipation in the second boundary layer is immaterial.

Case 2. Moderate separation between two reflection points

In figures 9–11 we keep the frequency at 1.9 Hz and the horizontal length of the slope at 4 m, but change the current velocity at the left edge to -0.13 m/s and at the right edge to -0.26 m/s. The current gradient is now $-0.033\ \mathrm{s}^{-1}$. This gives the dimensionless parameters $\epsilon = 0.11$ and $\Gamma = 0.0016$. The boundary condition at the left edge of each snapshot is given by (8.1) and (8.2), where $c = 0.15$. Starting with $T = 0$, the time interval between each consecutive snapshot is $\Delta T = 1.6$. In physical variables, $c^* \approx 3.1 \times 10^{-3}\ \mathrm{s}^{-2}$ and the time interval between each snapshot is approximately 11 s.

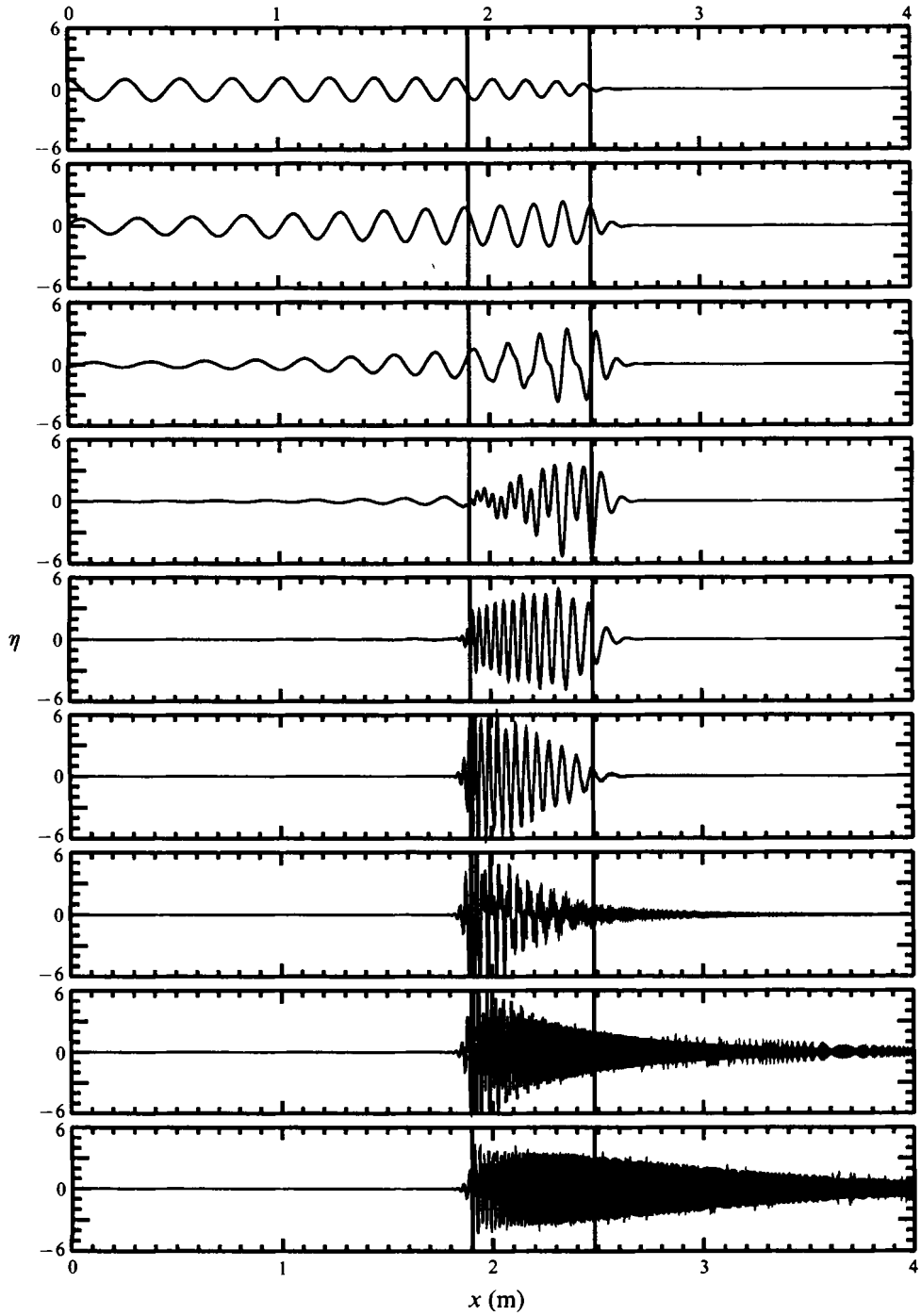

FIGURE 9. Double reflection with frequency 1.9 Hz and current gradient $-0.033\ \mathrm{s}^{-1}$. No damping.

Damping is added to the ray solutions in the same way as in case 1, which gives the same damping parameter χ. Because of the reduced separation, the wavepacket goes through the second reflection point before it is damped out, as is apparent from figure 10.

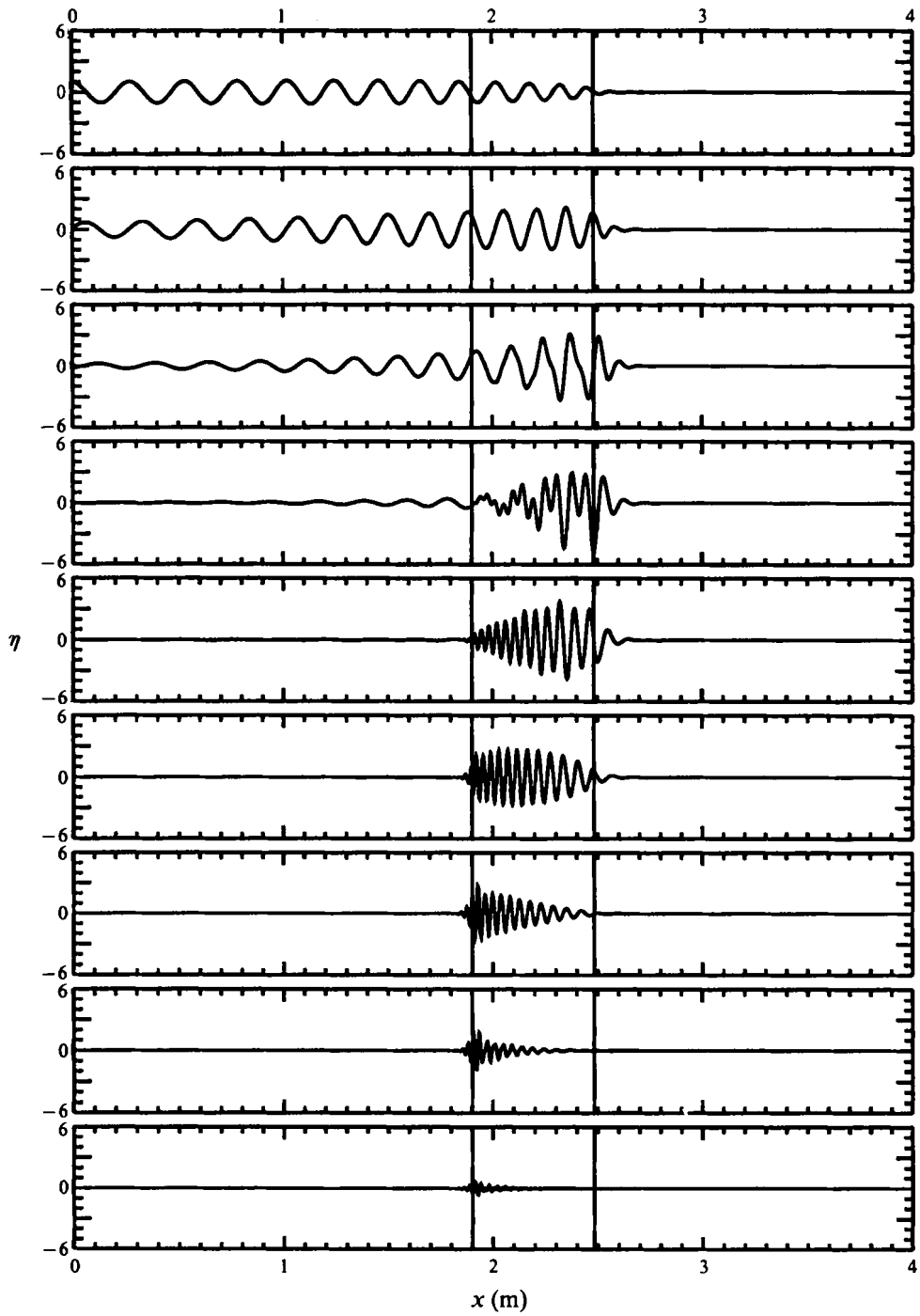

FIGURE 10. Double reflection with frequency 1.9 Hz and current gradient $-0.033\ s^{-1}$. Waves away from the reflection points are damped.

We also trace the peak of the envelope as a function of time in figure 11. After the first reflection, the envelope slows down considerably before being reflected the second time. We note that the characteristic times for viscous damping at the two reflection points are the same as in the previous case. However the times for propagation through

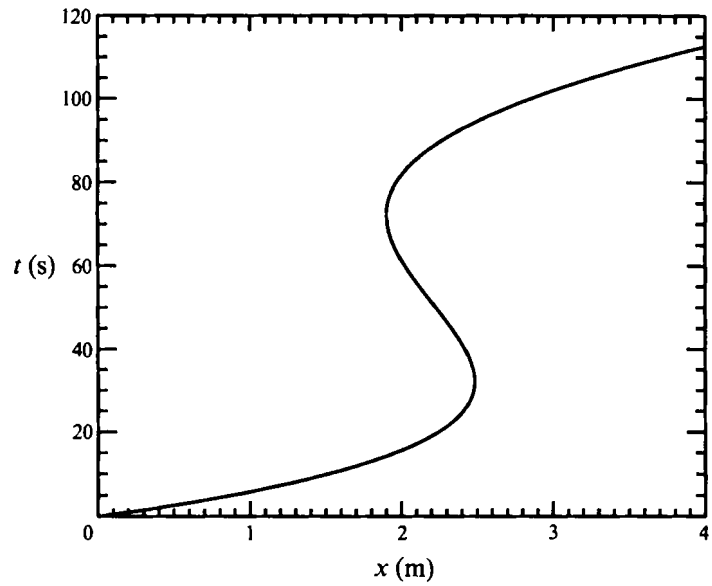

FIGURE 11. The trajectory of the envelope peak for frequency 1.9 Hz and current gradient $-0.033\ \mathrm{s}^{-1}$.

the reflection point boundary layers are now 20 s and 12 s, respectively. The effect of damping is now negligible at the (first) gravity reflection point, while it is significant but not of dominating importance at the capillary reflection point.

Case 3. Coalescing reflection points (triple turning point)

In this example, a wavepacket with the perfect triple turning point frequency (about 2.35 Hz) is considered, as shown in figure 12, here without viscous damping. We have used a linear current flowing from right to left, with the current velocity at the left edge being -0.15 m/s and at the right edge -0.21 m/s. The horizontal length across the figure is 3 m. The current gradient is $-0.02\ \mathrm{s}^{-1}$, and the long lengthscale should be about $L = 9$ m. This gives the dimensionless parameters $\epsilon = 0.071$ and $\Gamma = 0.0037$. The boundary condition at the left edge for consecutive snapshots is given by (8.1) and (8.2), where $c = 0.08$. Starting with $T = -2.8$, the time interval between consecutive snapshots is $\Delta T = 1.4$. In physical coordinates, this corresponds to $c^* \approx 4.4 \times 10^{-4}\ \mathrm{s}^{-2}$ and the time between consecutive snapshots is approximately 19 s.

As in the case of double reflection, the long incident gravity wave and the short transmitted capillary wave have speeds comparable to each other. However, it takes a considerable time for the wavepacket to go through the turning point. The trajectory of the peak of the wavepacket shown in figure 14 shows that the wavepacket comes almost to a standstill near the turning point. In physical units, the time spent in the inner region can be estimated at about 36 s, by using the inner scaling law (6.16) as before.

The characteristic time for viscous damping at the triple-root point can be estimated at about 48 s. In this case, viscous damping effects should be considerable in the boundary layer. However the theory for damping is difficult here since the region is small and the spatial variation of the wavelength is fast. With these reservations, we present in figure 13 the results with damping imposed only to waves away from the turning point. Even with this partial account taken of dissipation, waves are effectively annihilated near the triple point.

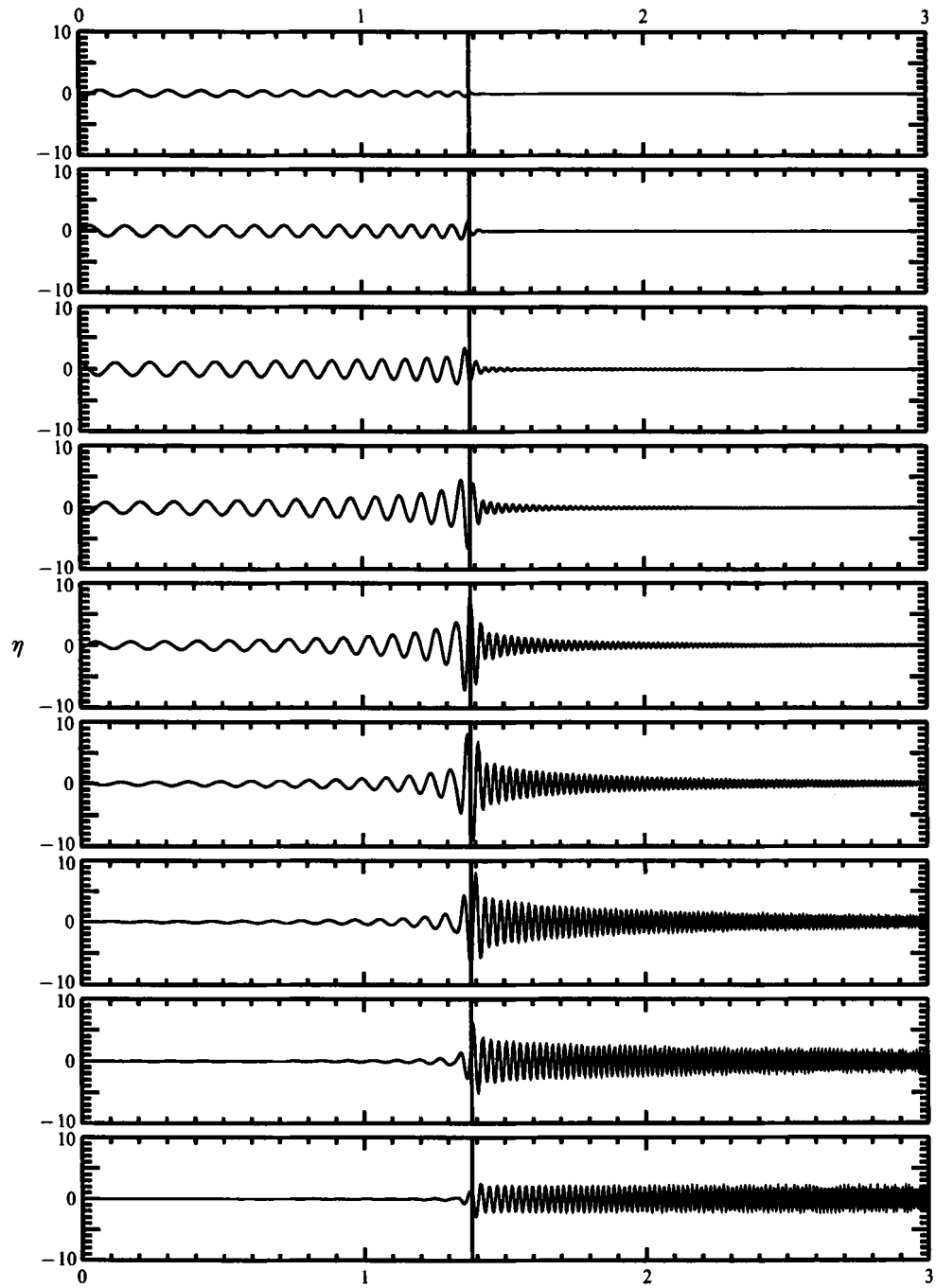

FIGURE 12. The perfect triple turning point with current gradient $-0.02\ s^{-1}$. No damping.

9. Conclusions

We have developed a linearized theory of waves propagating on an opposing current of increasing strength. Attention is focused on the effect of capillarity which makes it possible for repeated reflection. This process enhances the role of dissipation by

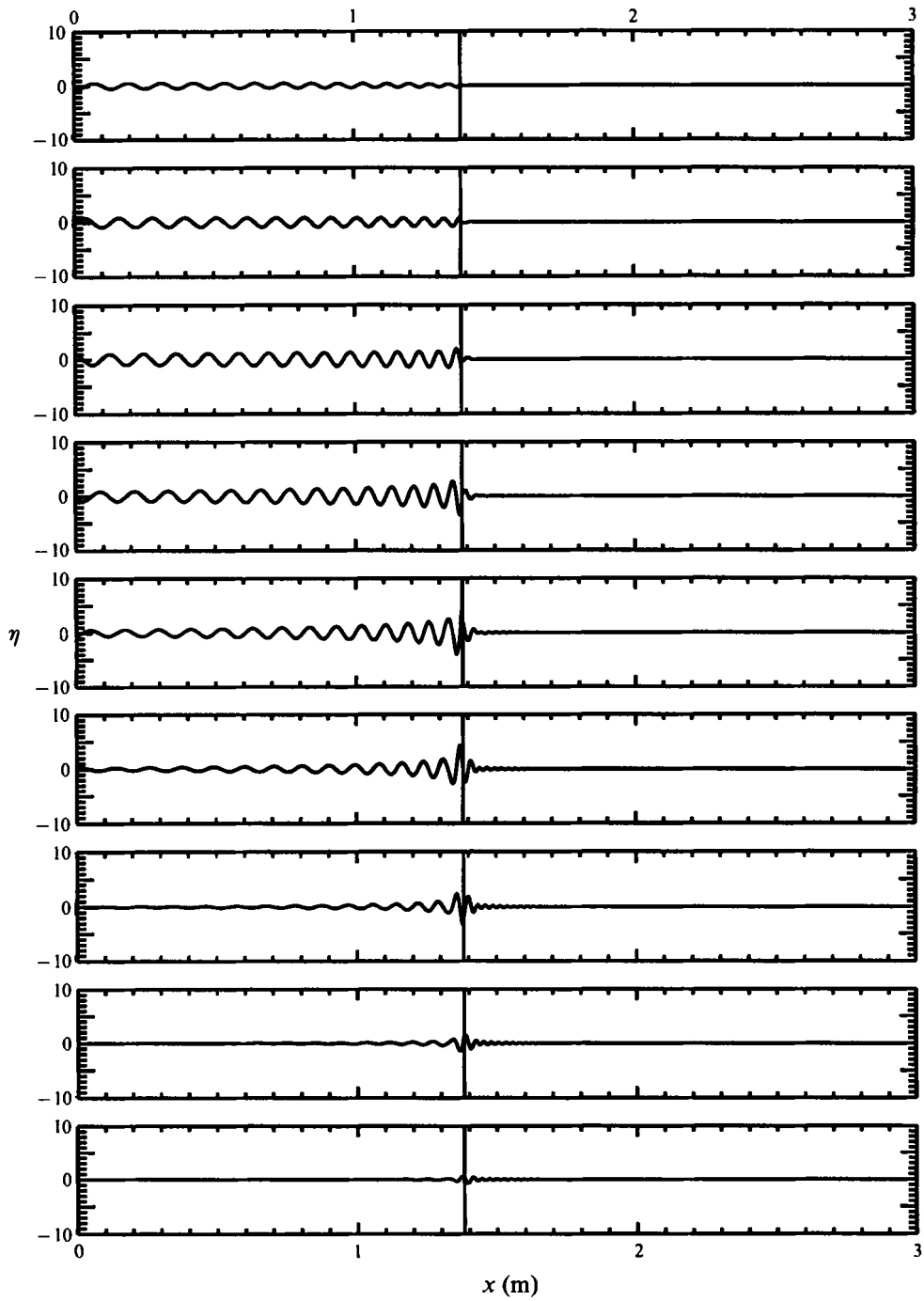

FIGURE 13. The perfect triple turning point with current gradient $-0.02\ \mathrm{s}^{-1}$. Waves away from the turning point are damped.

viscosity, which can damp out the waves completely without breaking. For a wavetrain of a given frequency, an increase of the current gradient narrows the region between the two reflection points. It is found that as the region gets narrower the wavepacket remains relatively longer within that region.

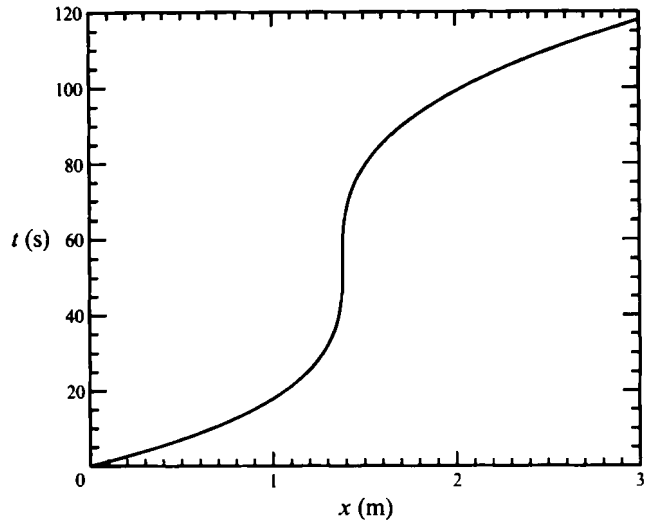

FIGURE 14. The trajectory of the envelope peak for the perfect triple turning point with current gradient $-0.02\ \mathrm{s}^{-1}$.

For comparison with future experiments, it may be desirable to include higher-order terms to allow moderate values of ϵ. In addition nonlinear and viscous effects deserve future attention. The role of nonlinearity may be treated by pursuing further the physical implications of the cubic Schrödinger equations derived in form by Peregrine & Smith (1979). Since the zone of a simple reflection point or a triple turning point is a thin boundary layer where the wavelength varies relatively rapidly, the treatment of viscosity is not trivial. In view of the present study, the effects of viscosity may also be of overwhelming importance.

We thank Dr Norden Huang for introducing us to the papers by Badulin *et al.* (1983) and Pokazeyev & Rozenberg (1983), which initiated this study. This research has been supported by The Norwegian Research Council for Science and the Humanities (NAVF 412.90/024) for a graduate Fellowship, US Office of Naval Research (contract N00014-90J-1163), and US National Science Foundation (Grant 9115689-CTS).

Appendix. Solution of the Pearcey equation

Consider equation (6.35)

$$\frac{\mathrm{d}^3 B}{\mathrm{d}\xi^3} - \frac{2\mathrm{i}K_0\sigma_0 U_1}{\Gamma_0}\xi B = 0, \tag{A 1}$$

where ξ is real, subject to the boundary conditions that B is bounded as $\xi \to \pm\infty$.

Let us introduce the coefficient of the wavenumber expansion (6.9)

$$\alpha = (-2K_0\sigma_0 U_1/\Gamma_0)^{\frac{1}{3}}, \tag{A 2}$$

and

$$Y = \sqrt{2}\alpha^{\frac{3}{4}}\mathrm{e}^{-\pi\mathrm{i}/8}\xi. \tag{A 3}$$

Equation (A 1) then becomes

$$\frac{\mathrm{d}^3 B}{\mathrm{d}Y^3} - \tfrac{1}{4}YB = 0. \tag{A 4}$$

The solution of (A 4) is a special case of the Pearcey function (Pearcey 1946),

$$P(Y) = \int_{-\infty}^{\infty} e^{-t^4+iYt}\,dt, \tag{A 5}$$

which has been discussed by Stamnes (1986) and Paris (1991). The integral above is a special case of Paris' equation (2.2) (scaled by a factor of $\exp(\pi i/8)$).

For $\xi > 0$, we have $\arg Y = -\frac{1}{8}\pi$. From (2.11) in Paris, we get

$$P(Y) \sim P_0 + P_1 \quad \text{for} \quad |\arg Y| < \tfrac{3}{8}\pi, \tag{A 6}$$

where P_m is the contribution from the saddle point at

$$t_m = 4^{-\frac{1}{3}} \exp\{\tfrac{1}{3}i(\tfrac{1}{2}\pi + \arg Y) + \tfrac{2}{3}\pi i m\}.$$

For large Y, the general expression for P_m is (cf. Paris' (2.14))

$$P_m(Y) \sim (\tfrac{1}{3}\pi)^{\frac{1}{2}} 2^{\frac{1}{6}} \exp\left\{\frac{3}{4^{\frac{4}{3}}} Y^{\frac{4}{3}} e^{2\pi i(1+m)/3}\right\} \times \left\{Y^{-\frac{1}{3}} e^{-\pi i/6 - 2\pi i m/3} - \frac{7}{36} 4^{\frac{1}{3}} Y^{-\frac{5}{3}} e^{\pi i/6 + 2\pi i m/3} + O(Y^{-\frac{7}{3}})\right\}. \tag{A 7}$$

For ease of reference, we shall display the first two terms of the derivative,

$$\frac{\partial P_m(Y)}{\partial Y} \sim (\tfrac{1}{3}\pi)^{\frac{1}{2}} 2^{\frac{1}{6}} \exp\left\{\frac{3}{4^{\frac{4}{3}}} Y^{\frac{4}{3}} e^{2\pi i/3 + 2\pi i m/3}\right\} \times \left\{4^{-\frac{1}{3}} e^{\pi i/2} - \frac{7}{36} Y^{-\frac{4}{3}} e^{-\pi i/6 - 2\pi i m/3} + O(Y^{-2})\right\}. \tag{A 8}$$

For ξ real, P_0 represents an algebraically damped oscillation, while P_1 is exponentially damped. Hence for purposes of asymptotic matching, only P_0 is needed.

REFERENCES

Badulin, S. I., Pokazeyev, K. V. & Rozenberg, A. D. 1983 A laboratory study of the transformation of regular gravity–capillary waves in inhomogeneous flows. *Izv. Atmos. Ocean. Phys.* **19** (10), 782–787.

Basovich, A. Y. & Talanov, V. I. 1977 Transformation of short surface waves on inhomogeneous currents. *Izv. Atmos. Ocean. Phys.* **13** (7), 514–519.

Bretherton, F. P. & Garrett, C. J. R. 1968 Wavetrains in inhomogeneous moving media. *Proc. R. Soc. Lond.* A **302**, 529–554.

Henyey, F. S., Creamer, D. B., Dysthe, K. B. Schult, R. L. & Wright, J. A. 1988 The energy and action of small waves riding on large waves. *J. Fluid Mech.* **189**, 443–462.

Lai, R. J., Long, S. R. & Huang, N. E. 1989 Laboratory studies of wave–current interaction: kinematics of the strong interaction. *J. Geophys. Res.* **94** (C11), 16201–16214.

Longuet-Higgins, M. S. & Stewart, R. W. 1960 Changes in the form of short gravity waves on long waves and tidal currents. *J. Fluid Mech.* **8**, 565–583.

Longuet-Higgins, M. S. & Stewart, R. W. 1961 The changes in amplitude of short gravity waves on steady non-uniform currents. *J. Fluid Mech.* **10**, 529–549.

Paris, R. B. 1991 The asymptotic behaviour of Pearcey's integral for complex variables. *Proc. R. Soc. Lond.* A **432**, 391–426.

Pearcey, T. 1946 The structure of an electromagnetic field in the neighbourhood of a cusp of a caustic. *Phil. Mag.* **37**, 311–317.

Peregrine, D. H. & Smith, R. 1979 Nonlinear effects upon waves near caustics. *Phil. Trans. R. Soc. Lond.* A **292**, 341–370.

PHILLIPS, O. M. 1981 The dispersion of short wavelets in the presence of a dominant long wave. *J. Fluid Mech.* **107**, 465–485.

POKAZEYEV, K. V. & ROZENBERG, A. D. 1983 Laboratory studies of regular gravity-capillary waves in currents. *Okeanologiya* **23** (4), 429–435.

SHYU, J.-H. & PHILLIPS, O. M. 1990 The blockage of gravity and capillary waves by longer waves and currents. *J. Fluid Mech.* **217**, 115–141.

SMITH, R. 1975 The reflection of short gravity waves on a non-uniform current. *Math. Proc. Camb. Phil. Soc.* **78**, 517–525.

STAMNES, J. J. 1986 *Waves in Focal Regions.* Adam Hilger.

STIASSNIE, M. & DAGAN, G. 1979 Partial reflexion of water waves by non-uniform adverse currents. *J. Fluid Mech.* **92**, 119–129.